

NBSIR 88-3773

Ignition and Flame Spread Measurements of Aircraft Lining Materials

Margaret Harkleroad

U.S. DEPARTMENT OF COMMERCE
National Bureau of Standards
National Engineering Laboratory
Center for Fire Research
Gaithersburg, MD 20899

May 1988



75 Years Stimulating America's Progress
1913-1988

Sponsored by:

**Federal Aviation Administration
Technical Center
Atlantic City, NJ 08405**

NBSIR 88-3773

**IGNITION AND FLAME SPREAD
MEASUREMENTS OF AIRCRAFT
LINING MATERIALS**

Margaret Harkleroad

U.S. DEPARTMENT OF COMMERCE
National Bureau of Standards
National Engineering Laboratory
Center for Fire Research
Gaithersburg, MD 20899

May 1988

Sponsored by:
Federal Aviation Administration
Technical Center
Atlantic City, NJ 08405



U.S. DEPARTMENT OF COMMERCE, C. William Verity, *Secretary*
NATIONAL BUREAU OF STANDARDS, Ernest Ambler, *Director*

TABLE OF CONTENTS

	<u>Page</u>
LIST OF TABLES	iv
LIST OF FIGURES	v
ABSTRACT	1
INTRODUCTION	2
Purpose	2
Background	2
Objective	3
DISCUSSION	5
Ignition and Lateral Flame Spread Results	5
Apparatus	5
Ignition	5
Flame Spread	7
Flame Height and Flame Heat Transfer on Vertical Walls	10
Apparatus	10
Test Results and Analysis	10
CONCLUSIONS	15
ACKNOWLEDGMENTS	15
REFERENCES	16
NOMENCLATURE	17

LIST OF TABLES

	<u>Page</u>
Table 1. Aircraft panel descriptions	4
Table 2. Ignition parameters	7
Table 3. Flame spread parameters in terms of radiant flux	8
Table 4. Lateral flame spread parameters	9
Table 5. Parameters significant toupwarde flame spread	12
Table 6. Upward flame spread parameters	15

LIST OF FIGURES

		<u>Page</u>
Figure 1.	Schematic of ignition and flame spread apparatus	19
Figure 2.	Normalized irradiance over the specimen	19
Figure 3.	Correlation of ignition and flame spread results for the epoxy fiberglass panel	20
Figure 4.	Correlation of ignition and flame spread results for the phenolic fiberglass panel	21
Figure 5.	Correlation of ignition and flame spread results for the epoxy kevlar panel	22
Figure 6.	Correlation of ignition and flame spread results for the phenolic kevlar panel	23
Figure 7.	Correlation of ignition and flame spread results for the phenolic graphite panel	24
Figure 8.	Correlation of ignition and flame spread results for the ABS panel	25
Figure 9.	Correlation of ignition and flame spread results for the polycarbonate panel	26
Figure 10.	Correlation of ignition and flame spread results for the ULTEM panel	27
Figure 11.	Equilibrium surface temperatures as a function of external radiant heating in the test apparatus	28
Figure 12.	Schematic of heat transfer apparatus	28
Figure 13.	Flame spread problem	29
Figure 14.	Procedure for determining average peak burning values	29
Figure 15-A.	Flame heat transfer to vertical wall above panel with epoxy/fiberglass facing	30
Figure 15-B.	Flame height from base of burning panel with epoxy/fiberglass facing	30
Figure 16-A.	Flame heat transfer to vertical wall above panel with phenolic/fiberglass facing	31
Figure 16-B.	Flame height from base of burning panel with phenolic/fiberglass facing	31

LIST OF FIGURES (continued)

	<u>Page</u>
Figure 17-A. Flame heat transfer to vertical wall above panel with epoxy/kevlar facing	32
Figure 17-B. Flame height from base of burning panel with epoxy/kevlar facing	32
Figure 18-A. Flame heat transfer to vertical wall above panel with phenolic/kevlar facing	33
Figure 18-B. Flame height from base of burning panel with phenolic/kevlar facing	33
Figure 19-A. Flame heat transfer to vertical wall above panel with phenolic/graphite facing	34
Figure 19-B. Flame height from base of burning panel with phenolic/graphite facing	34
Figure 20-A. Flame heat transfer to vertical wall above ABS panel	35
Figure 20-B. Flame height from base of burning ABS panel	35
Figure 21-A. Flame heat transfer to vertical wall above polycarbonate panel	36
Figure 21-B. Flame height from base of burning polycarbonate panel	36
Figure 22-A. Flame heat transfer to vertical wall above ULTEM panel	37
Figure 22-B. Flame height from base of burning ULTEM panel	37
Figure 23. Wall heat flux distribution for epoxy/fiberglass panel	38
Figure 24. Wall heat flux distribution for phenolic/fiberglass panel	39
Figure 25. Wall heat flux distribution for epoxy/kevlar panel	40
Figure 26. Wall heat flux distribution for phenolic/kevlar panel	41
Figure 27. Wall heat flux distribution for phenolic/graphite panel ...	42
Figure 28. Wall heat flux distribution for ABS panel	43
Figure 29. Wall heat flux distribution for polycarbonate panel	44
Figure 30. Wall heat flux distribution for ULTEM panel	45
Figure 31. Wall heat flux in terms of x/x_f	46

LIST OF FIGURES (continued)

	<u>Page</u>
Figure 32. Peak energy release rate under external irradiance	47
Figure 33. Peak energy release rate for epoxy/fiberglass panel	48
Figure 34. Peak energy release rate for phenolic/fiberglass panel	49
Figure 35. Peak energy release rate for epoxy/kevlar panel	50
Figure 36. Peak energy release rate for phenolic/kevlar panel	51
Figure 37. Peak energy release rate for phenolic/graphite panel	52
Figure 38. Peak energy release rate for ABS panel	53
Figure 39. Peak energy release rate for polycarbonate panel	54
Figure 40. Peak energy release rate for ULTEM panel	55

Abstract

Experimental tests have been conducted to study the lateral and upward flame spread behavior of eight aircraft lining materials; three advanced thin panels (ABS, polycarbonate and ULTEM) and five panels of a honeycomb cell structure covered with varying facings (epoxy/fiberglass, phenolic/fiberglass, epoxy/kevlar, phenolic/kevlar and phenolic/graphite). The state-of-the-art experimental and analytical procedures are succinctly described in this paper, but previously they have been expounded fully in the indicated references. The results have been tabulated in terms of parameters useful in predicting ignition and flame spread behavior in the presence of an ignition source under exposure from an external radiant source. Experimental and derived results are graphically compared. Supplemental ignition, spread, heat transfer and energy release rate results have been included. Derived material properties related to and indicative of the propensity to support flame spread are presented.

Key words: ignition; flame spread; aircraft interiors; material properties

INTRODUCTION

PURPOSE.

The purpose of this study was to provide the Federal Aviation Administration (FAA) with information on the flammability of aircraft cabin interior panel materials.

BACKGROUND.

Experimental data on eight aircraft interior panel materials are to be derived from measurements made with the flame spread and the heat (energy) release rate apparatuses at the National Bureau of Standards (NBS). These results would supplement additional experimental data from FAA on the panels involving their performances in laboratory, model-scale and full-scale experiments.

Post-crash aircraft fire experiments have shown flashover, the event in which fire growth beyond a localized region of combustion is rapid and extensive, to be the most significant factor affecting survival and escape time. It is therefore important to understand the flame spread and combustion characteristics of cabin materials and their role in promoting flashover. State-of-the-art fire science and technology suggest the feasibility of experimentally identifying the mechanics responsible for flashover and relating it to the contribution of a particular furnishing material. Thus from the observation of fire development and appropriate material data, it is possible to analyze a particular material in terms of its contribution to flashover. For

wall and carpet materials, the measurement of their ignition, flame spread properties, and mass loss and energy release rate should completely characterize their contribution. While predictive methods for fire growth in terms of laboratory test data are still in the developmental stages, it might be useful to analyze and correlate full scale results in terms of these data. Thus, if ignition is assessed to be critical in a specific fire scenario, then ignition characteristics alone will serve to evaluate a material's performance. Experiments can then be analyzed to seek clues in developing correlations with test data.

OBJECTIVE.

The objectives of this study were to examine the performance of selected aircraft panel materials (5 honeycomb and 3 thin) under piloted ignition as a function of external radiation for their ignition and flame spread properties. Parameters relevant to these phenomena were to be derived from experimental ignition, flame spread and heat transfer data. Since the test procedures and their theoretical analysis have been fully described by Harkleroad, Quintiere et al. (references 1, 2, and 3) only the end results are to be presented. For comparison purposes, results from previous tests (reference 4) of five honeycomb panels with different laminated coverings and additional data taken for those panels in this series of tests are to be included. The materials are described in Table 1.

TABLE 1. AIRCRAFT PANEL DESCRIPTIONS*

<u>Sample Name</u>	<u>Description</u> *
Epoxy fiberglass	Epoxy glass facings, face and back 1 ply 7781 style woven fiberglass impregnated with epoxy resin, fire retardant, and co-cured to 1/8 cell Nomax® honeycomb. One surface to be covered with 2 mil white Tedlar®.
Phenolic fiberglass	Phenolic glass facings, face and back 1 ply 7781 type woven fiberglass impregnated with a modified phenolic resin, and co-cured to 1/8 Nomex honeycomb. One surface to be covered with 2 mil white Tedlar.
Epoxy Kevlar®	Epoxy Kevlar facings, face and back 1 ply 285 style woven Kevlar impregnated with epoxy resin fire retardant, and co-cured to 1/8 cell Nomex honeycomb. One surface to be covered with 2 mil white Tedlar.
Phenolic Kevlar	Phenolic Kevlar facings, face and back 1 ply 285 style woven kevlar impregnated with a modified phenolic resin and co-cured to 1/8 cell Nomex honeycomb. One surface to be covered with 2 mil white Tedlar.
Phenolic graphite	Phenolic graphite facings, 1 ply 8 harness satin, 3 K fiber T-300 woven graphite impregnated with a modified phenolic resin, and co-cured to 1/8 cell Nomex honeycomb. One surface to be covered with 2 mil white Tedlar.
ABS	A 0.06 inch panel composed of 80% acrylonitriol-butadiene-styrene and 20% PVC.
Polycarbonate	A 0.06 inch polycarbonate of polyetherimide-resin.
ULTEM®	A 0.06 inch panel.

*The use of trade names are for descriptive purposes only and should not be construed as endorsement by the National Bureau of Standards or the Federal Aviation Administration.

DISCUSSION

IGNITION AND LATERAL FLAME SPREAD RESULTS.

APPARATUS. The apparatus for examining radiative ignition and flame spread is essentially the apparatus developed by Robertson (reference 5). It consists of a radiant heat source, a sample holder, and a pilot flame to promote ignition. A schematic of the arrangement is shown in figure 1. A steel plate is positioned above the sample to extend the sample surface and enable the boundary layer containing the pyrolyzed gases and the induced air flow to be maintained above the sample. An acetylene-air pilot flame interrupts this boundary layer mixture insuring ignition based on the mixture concentration generated at the sample surface. The radiant heat flux distribution to the sample surface, normalized in terms of incident flux at $x = 50$ mm, is shown in figure 2.

IGNITION. Ignition tests were conducted by exposing the panel surface to an incident flux (q''_e) that varied from 1.5 to 6.5 W/cm² and recording the time to ignite. A minimum flux necessary for ignition ($q''_{o,ig}$) is experimentally determined as the limit at which no ignition occurs. The approach used in the ignition analysis is based on steady-state energy balance which holds after long heating (references 2, 6) and is represented by the expression

$$q''_{o,ig} = h_c (T_{ig} - T_s) + \epsilon \sigma (T_{ig}^4 - T_s^4) = h (T_{ig} - T_s) \quad (1)$$

where T_{ig} represents the ignition temperature, T_s the ambient temperature, h_c the convective heat transfer coefficient, σ the surface absorbency and ϵ the emissivity.

The ignition time (t), for the cases in which the incident flux is great enough to ignite the material, is correlated in terms of

$$\frac{q''_{o,ig}}{q''_e} = F(t) = \begin{cases} b\sqrt{t}, & t \leq t_m \\ 1, & t \geq t_m \end{cases} \quad (2)$$

where $F(t)$ is a time-response function representing the thermal response of the material to external radiation, b is a material constant and t_m is a characteristic time indicative of the thermal equilibrium time (references 2, 6). The ignition data with the correlated results indicated by the solid line are shown in figures 3-10. Quintiere (reference 2) has shown that the parameter b can be used to compute an effective material $k\rho c$ from the expression

$$k\rho c = 4/\pi (h/b)^2 \quad (3)$$

where h , a heat transfer coefficient, is determined at the ignition temperature (T_{ig}). Ignition temperatures (T_{ig}) can be found from the theoretical curve of figure 11 which expresses the surface temperature of a material, under long heating conditions in the apparatus, as a function of external radiant flux (reference 2, 6, 8). Ignition parameters for the three thin and the five honeycomb panels are listed in Table 2.

TABLE 2. IGNITION PARAMETERS

Aircraft Panel	$q''_{o,ig}$ (W/cm ²)	T _{ig} (°C)	b (s ^{-1/2})	t _m (s)	$k\rho c$ $\left(\frac{kW}{m^2K}\right)^2s$
ABS	1.6	388.	0.073	188.	0.76
epoxy/fiberglass	2.0	438.	0.132	58.	0.174
epoxy/kevlar	2.3	465.	0.135	55.	0.188
polycarbonate	2.9	518.	0.072	190.	0.84
phenolic/kevlar	3.4	558.	0.196	26.	0.133
phenolic/fiberglass	3.6	570.	0.227	19.	0.107
phenolic/graphite	3.6	570.	0.72	34.	0.186
ULTEM	3.8	585.	0.08	156.	0.91

FLAME SPREAD. Opposed flow spread results were obtained from tests conducted with the panel (mounted as indicated in figure 1) exposed to a known external radiant flux (q''_e), ignited by a pilot flame and noting the lateral flame spread position (x_p) as a function of time (t). These flame spread results are applicable to opposed flow flame spread on a vertical surface where the flame provides a constant heat flux that influences the opposed flow (reference 1). The spread velocity (V) is expressed in terms of the external radiant flux (q''_e) from the flux distribution curve of figure 2 and time (t).

$$V = \frac{dx_p}{dt} \text{ vs } q''_e(x_p(t)). \quad (4)$$

It has been shown (references 1, 2, 6) that flame spread for a material under thermal equilibrium can be correlated by the expression

$$V^{-1/2} = C [q''_{o,ig} - q''_e F(t)]; \text{ for } q''_{o,s} \leq q''_e F(t) \leq q''_{o,ig} \quad (5)$$

where C is a material flame heat transfer factor, $q''_{o,ig}$ is the minimum flux necessary for ignition, $F(t)$ is the time response factor and $q''_{o,s}$ is the maximum flux necessary for spread derived from the flame propagation limit. Equation 5 is valid when the minimum flux required to propagate spread ($q''_{o,s}$) is greater than the product of the externally applied flux (q''_e) and the time function $f(t)$, and this product is greater than the minimum flux necessary for ignition. A minimum flux for flame spread, $q''_{o,s}$, can be derived from the flame propagation limit and figure 2 (reference 1). The measured spread velocities, with the correlated results indicated by the dashed line are shown in figures 3-8 for the condition where the material is under an external irradiance a sufficient time to reach thermal equilibrium. While spot ignition was observed at protruding surfaces, insufficient spread occurred overall to calculate accurate flame spread results for the polycarbonate and ULTEM panels. The polycarbonate panel melted forming various shapes and sizes and pulled away from the holder. The ULTEM bubbled, melted, and charred. Flame spread parameters in terms of radiant flux are listed in Table 3.

TABLE 3. FLAME SPREAD PARAMETERS IN TERMS OF RADIANT FLUX

Aircraft Panel	$q''_{o,ig}$ (W/cm ²)	C $\left(\frac{s}{mm}\right)^{1/2} \left(\frac{cm^2}{W}\right)$	$q''_{o,s}$ (W/cm ²)
ABS	1.9	1.9	0.93
epoxy/fiberglass	2.1	2.5	1.90
epoxy/kevlar	2.4	1.20	1.70
polycarbonate	NS	NS	NS
phenolic/kevlar	3.5	1.16	2.8
phenolic/graphite	3.7	0.97	2.8
phenolic/fiberglass	3.8	0.63	2.6
ULTEM	NS	NS	NS

NS indicates no flame spread

Flame spread can also be represented by the expression

$$V = \frac{\phi}{k\rho c (T_{ig} - T_s)^2}, \text{ for } T_{s,m} \leq T_s \leq T_{ig} \quad (6)$$

where ϕ is an empirical parameter representing the gas phase properties, flame temperature, opposed flow gas velocity and chemical kinetic effects usually denoted a Damkohler number (reference 2). The related flame spread parameters are tabulated in Table 4. Here T_{ig} is derived from the sample's ignition data, that is, from Table 2.

TABLE 4. LATERAL FLAME SPREAD PARAMETERS

Aircraft Panel	T_{ig} (°C)	$k\rho c$ $\left(\frac{kW}{2m^2K}\right)^2 s$	ϕ $\frac{(kW)^2}{m^3}$	$T_{s,min}$ (°C)
ABS	388.	0.76	6.63	282.
epoxy/fiberglass	438.	0.174	1.17	425.
epoxy/kevlar	465.	0.188	4.86	400.
polycarbonate	518.	0.84	NS	518.
phenolic/kevlar	558.	0.133	2.47	510.
phenolic/fiberglass	570.	0.107	6.23	490.
phenolic/graphite	570.	0.186	4.58	510.
ULTEM	585.	0.91	NS	585.

NS indicates no flame spread

The flame spread "properties" listed in Table 3 depend on the apparatus/environmental conditions. Those listed in Table 4 are correlation parameters defined from the flame spread model. They are more generic properties and approximate the underlying physical-chemical properties. In both cases, these properties have been determined under natural convection conditions in normal air. For other conditions at least the ϕ parameter would

change -- for example, it depends on the gas velocity and ambient oxygen concentration.

FLAME HEIGHT AND FLAME HEAT TRANSFER ON VERTICAL WALLS

APPARATUS. Flame height and flame heat transfer tests were conducted with a sample flush-mounted below a water-cooled instrumented copper plate, exposed to an external irradiant flux (q''_e) that varied from 1 to 4 W/cm², and ignited with a line burner positioned below the sample. A schematic of the apparatus is shown in figure 12. Total heat flux (q''_x) was recorded by water cooled heat flux sensors embedded in the copper plate at six locations above the sample. The flame heat flux (q''_f) was determined by subtracting the recorded external radiant flux. Flame heights (x_f), defined as the uppermost position of the luminous flame, were determined from video records.

TEST RESULTS AND ANALYSIS. Figure 13 schematically depicts the approach used in analyzing the flame spread problem. Here, the region over which pyrolysis has ceased is indicated by x_b and the time for this burnout, i.e., the duration of the pyrolysis, by t_b . The pyrolysis height, i.e., the region undergoing pyrolysis is represented by x_p , the flame height by x_f , and the time for spread over the flame heat transfer region by t_f .

Peak burning values were obtained by an arbitrarily selected data averaging procedure shown in figure 14 for the heat flux vs time curve of the epoxy kevlar panel under an external irradiance of 3 W/cm². Average peak heat fluxes and flame heights were determined for the time period representing 80 percent of the maximum values recorded. Similarly, the time that bounds 10

percent of the peak flux defines the burn time (t_b). This burn time will change as the material thickness changes.

The approach used for expressing upward flame spread velocity on a vertical surface is from reference 3 and is represented as

$$v = \frac{[q_f'']^2 [x_f - x_p]}{k\rho c [T_{ig} - T_s]^2} \quad (7)$$

or

$$v = \frac{x_f - x_p}{t_f} \quad (8)$$

where q_f'' represents the flame heat flux; x_f the flame height; x_p the pyrolysis height, T_{ig} and T_s the ignition and surface temperatures, respectively; $k\rho c$ the material thermal property; and t_f the time for spread over the flame heat transfer region ($x_f - x_p$) where

$$t_f = k\rho c [(T_{ig} - T_s)/q_f'']^2. \quad (9)$$

While an understanding of upward spread behavior is incomplete, these results suggest some tendencies for evaluating the problem. In evaluating the condition necessary for sustained propagation, the ratio of t_f/t_b may be significant since the burning time, t_b , must be long relative to t_f in order for spread to occur. Nominal spread rates computed from eq. 8 are similar in magnitude to the opposed flow maximum spread rate in figures 3-10. A summary of the results for upward spread are included in Table 5. Scatter in the flame heat flux data for the honeycomb panels is indicative of the random

TABLE 5. PARAMETERS SIGNIFICANT TO UPWARD FLAME SPREAD

	80% External Flux (q''_e) (W/cm ²)	80% Flame Flux (q''_e) (W/cm ²)	Flame Length (x_f) (cm)	Spread Time (t_f) (s)	Burn Time (t_b) (s)	Flame Heat Transfer Length ($x_f - x_p$) (cm)	Nominal Spread Rate, (Eq. (8)) $V = \frac{dx_p}{dt}$ (mm/s)
epoxy	2.0	1.1	48.	249.	80.	20.	0.8
fiberglass	2.5	1.3	58.	178.	100.	30.	1.7
	3.0 ^a	2.6	NV	45	88.	NV	NV
	3.1	2.2	60.	62	80.	32.	5.2
	3.4 ^a	2.0	48.	75.	60.	20.	2.7
	3.5	2.4	52.	52.	25.	24.	4.6
	3.8 ^a	0.9	61.	372.	29.	33.	0.9
phenolic	2.5	1.6	38.	124.	25.	10.	0.8
fiberglass	3.0	1.9	66.	88.	25.	38.	4.3
	3.4	1.6	56.	124.	55.	28.	2.3
	3.5	2.0	60.	80.	75.	32.	4.0
	3.8 ^d	0.8	90.	497.	43.	62.	1.2
epoxy	2.0	1.6	66.	144.	115.	38.	2.6
kevlar	2.0	2.0	49.	92.	135.	21.	2.3
	2.5	1.1	48.	305.	115.	20.	0.6
	3.0 ^e	0.9	57.	455.	115.	29.	0.6
	3.0	2.1	45.	84.	75.	17.	2.0
	3.3	2.0	50.	92.	77.	22.	2.4
	3.4	1.8	48.	114.	75.	20.	1.8
	3.7	1.7	89.	128.	101.	61.	4.8
	3.8	1.6	64.	144.	115.	36.	2.5
phenolic	2.5	1.6	54.	149.	364.	26.	1.7
kevlar	3.0	2.1	54.	87.	30.	26.	3.0
	3.0 ^b	1.4	66.	195.	28.	38.	1.9
	3.4	2.0	100.	96.	68.	72.	7.5
	3.6	4.3	58.	21.	66.	30.	14.3
	3.7 ^b	2.7	61.	52.	101.	33.	6.3
phenolic	2.0	1.0	40.	556.	29.	12.	0.2
graphite	2.5	2.1	42.	126.	83.	14.	1.1
	3.0 ^b	1.1	53.	459.	29.	25.	0.5
	3.0	2.1	55.	126.	96.	27.	2.1
	3.4 ^a	1.5	55.	126.	96.	27.	2.1
	3.4	2.1	63.	121.	75.	25.	2.1
	3.7 ^c	1.0	66.	556.	29.	38.	0.7
ABS	2.6	3.6	89.	79.	96.	61.	7.7
	3.1	3.4	102.	88.	96.	74.	8.4
	3.3	3.2	95.	99.	96.	67.	6.8
polycarbonate	2.6	1.4	49.	1054.	63.	21.	0.2
	3.0	2.5	63.	331.	124.	35.	1.1
	3.4	1.8	60.	638.	83.	32.	0.5
ULTEM	2.6	1.0	34.	2844.	39.	6.	0.02
	3.1	1.1	42.	2350.	204.	14.	0.06
	3.4	0.7	39.	5803.	55.	11.	0.02

NV indicates no video

^afacing peels upward covering lower sensor

^bpart of facing fell from sample

^cfacing exploded, burning only at edges

^dburning limited to lower edge of panel

^eburning extinguished and then re-ignited

unravelling process of the facing when heated. The heat transferred to the flux sensors was dictated by the decomposition of the facing which was observed to unravel upward and cover the lower sensor, unravel to the side directing the hot gases away from the sensors and to disintegrate with some sections falling away from the sample. Scatter in the flame heat flux data of the thin panels is indicative of their melting and dripping behavior.

Typical measured flame heat flux results are shown in figures 16-22, series A, for the panels under an external irradiance of 3 W/cm. Figures 16-22, series B, show corresponding measured flame heights. The data are analyzed in terms of the wall heat flux distributions shown in figures 23-30. The panels showed a decreasing flux distribution with distance measured from the base of the fire (bottom scale). This distance is normalized with the flame height (top scale) and the data are replotted in those figures as an attempt to coalesce the results into a general correlation. The solid line indicates Hasemi's data from reference 3 for a correlation of gaseous fuel heat transfer results along walls. Data for the eight panels are collectively shown in figure 31. For the most part, the data tend to group around the curve representing Hasemi's data.

Energy release rates (E''), based on flame height were derived from the expression

$$x_f = k_f (E'')^{2/3}. \quad (10)$$

from references 3 and 10. Here E'' is the energy release rate per unit flame width and k_f is the experimentally derived constant ($0.0569 \text{ m}/(\text{kW}/\text{m})^{2/3}$) from Hasemi's CH_4 line burner data. A comparison of the peak energy release rate

for the panels at varying external irradiances is shown in figure 32. The curves represent a least square fit of the data shown in figures 33-40. The solid portion of the line indicates the range for which ignition would be expected to occur based on the results of Table 2. (Lower values for the critical heat flux for ignition than shown in Table 2 are probably due to orientation differences and the bottom pilot flame in the vertical heat transfer apparatus).

A propagation parameter (μ) indicative of flame spread capability can be expressed in terms of energy release rate (E''), flame temperature (t_f) and burn time (t_b); Quintiere (reference 3), Williams (reference 10). This propagation parameter (μ) is derived from the expression

$$\mu = aE'' - t_f/t_b - 1 \quad (11)$$

from the work of Quintiere and

$$\mu = aE'' t_b/2t_f - 2/\pi \quad (12)$$

from the work of Williams. These theoretical results suggest that sustained flame spread propagation will occur for values of $\mu \geq 0$.

Measured and derived flame spread parameters are listed in Table 6 for a nominally fixed irradiance of 3 W/cm^2 .

TABLE 6. UPWARD FLAME SPREAD PARAMETERS

Aircraft Panel	q''_e (W/cm ²)	t_f^+ (s)	t_b (s)	E'' (kW/m ²)	μ Eq. (11)	μ Eq. (12)
ABS	3.1	127.	96.	285.	0.52	0.62
epoxy fiberglass	3.0	38.	88.	140.	- 0.03	0.37
epoxy kevlar	3.0	46.	77.	140.	- 0.20	0.15
polycarbonate	3.0	258.	124.	190.	- 1.18	- 0.20
phenolic kevlar	3.0*	48.	30.	140.	- 1.2	- 0.35
phenolic fiberglass	3.0*	40.	25.	140.	- 1.2	- 0.35
phenolic graphite	3.0*	70.	27.	140.	- 2.19	- 0.51
ULTEM	3.1*	372.	204.	55.	- 2.27	- 0.84

* critical ignition flux not exceeded

+ calculated for $q''_f = 25 \text{ kW/m}^2$, see Eq. (9)

CONCLUSION

Results useful in the prediction of opposed flow flame spread on vertical surfaces are tabulated in Tables 2, 3, and 4 for the eight aircraft lining materials studied. Parameters indicative of their propensity for and properties related to upward flame spread are shown in Tables 5 and 6. Some of these data relate to bulk properties associated with the particular material tested and correspond to the theoretical correlating models for flame spread. Other data presented, such as flame height and flame heat flux, depend on the scale of the experiment and the fire dynamics in general.

ACKNOWLEDGMENTS

The author is indebted to Dr. J. Quintiere for his technical assistance and guidance in the data analysis and to B. Rinkinen and D. Waggoner for their assistance in conducting the experimental tests.

REFERENCES

1. Harkleroad, M., Quintiere, J. and Walton, W., "Radiative Ignition and Opposed Flow Flame Spread Measurements on Materials", U.S. Department of Transportation, Fed. Aviation Admin. Tech. Ctr., DOT/FAA/CT83/28, August 1983.
2. Quintiere, J. and Harkleroad, M., "New Concepts for Measuring Flame Spread", Symp. on Applications of Fire Science to Fire Engineering, Amer. Soc. Testing and Materials/Soc. Fire Prot. Engrs., Denver, CO, June 26-27, 1984.
3. Quintiere, J., Harkleroad, M. and Hasemi, J., "Wall Flames and Implications for Upward Flame Spread", AIAA Paper No. 85-0456, 1985.
4. Quintiere, J., Babrauskas, V., Cooper, L., Harkleroad, M., Steckler, K. and Tewarson, A., "The Role of Aircraft Panel Materials in Cabin Fires and Their Properties", U.S. Dept. Trans., Fed. Aviation Admin. Tech. Ctr., DOT/FAA/CT-84-30, 1985.
5. Robertson, A.F., "A Flammability Test Based on Proposed ISO Spread of Flame Test", Third Progress Report, Intergovernmental Maritime Consultative Organization, IMCO FP/215, 1979.
6. Quintiere, J., *Fire and Materials*, Vol. 5, No. 2, 1981, pp. 52-60.
7. Babrauskas, V., "Development of the Cone Calorimeter - A Bench Scale Heat Release Rate Apparatus Panel on Oxygen Consumption", *Nat. Bur. Stand.*, NBSIR 82-2611, November 1982.
8. Quintiere, J., Harkleroad, M. and Walton, D., *Comb. Sci. and Technol.*, 1983, Vol. 32.
9. Sibulkin, M. and Kim, J., *Comb. Sci. and Technol.*, 1977, Vol. 17. pp. 39-49.
10. Saito, K., Williams, F.A. and Quintiere, J., "Upward Turbulent Flames", International Symposium on Fire Safety Science, 1985.

NOMENCLATURE

b	parameter in eq. (2)
c	specific heat
C	parameter in eq. (5)
E''	energy release rate per unit flame width
$F(t)$	thermal time-response function
h	heat loss coefficient
h_c	convective heat transfer coefficient
k	thermal conductivity
k_f	constant in eq. (10)
q''_e	external radiant flux
q''_f	flame heat flux
$q''_{o,ig}$	critical flux of ignition
$q''_{o,s}$	critical flux for spread
t	time
t_b	pyrolysis burn time
t_f	time for spread over heat transfer region
t_m	characteristics equilibrium time
T_{ig}	ignition temperature
T_s	surface temperature before flame effects
$T_{s,m}$	minimum temperature for spread
V	flame velocity
x_f	flame height
x_p	lateral flame position in eq. (4)
x_p	pyrolysis height in eqs. (7, 8)
ρ	density

ϵ emissivity
 σ Stefan-Boltzmann constant
 Φ parameter in eq. (6)
 μ parameter in eqs. (11, 12)

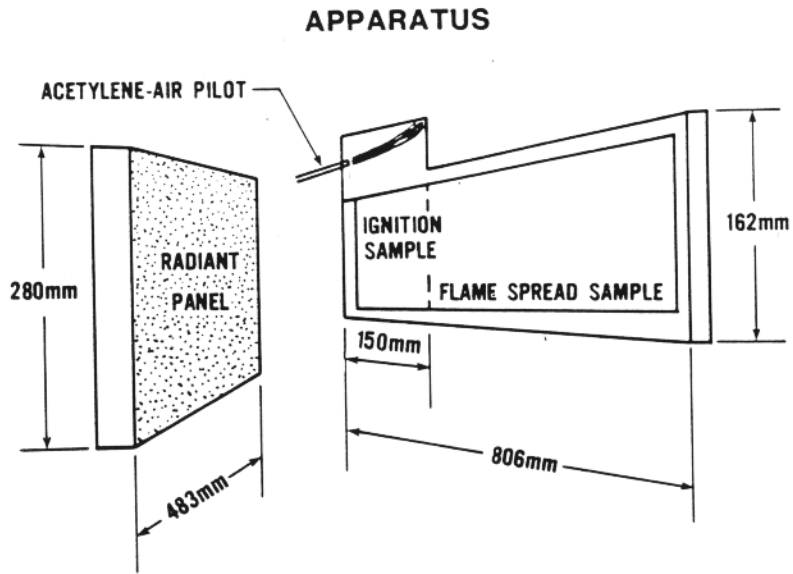


Figure 1. Schematic of ignition and flame spread apparatus.

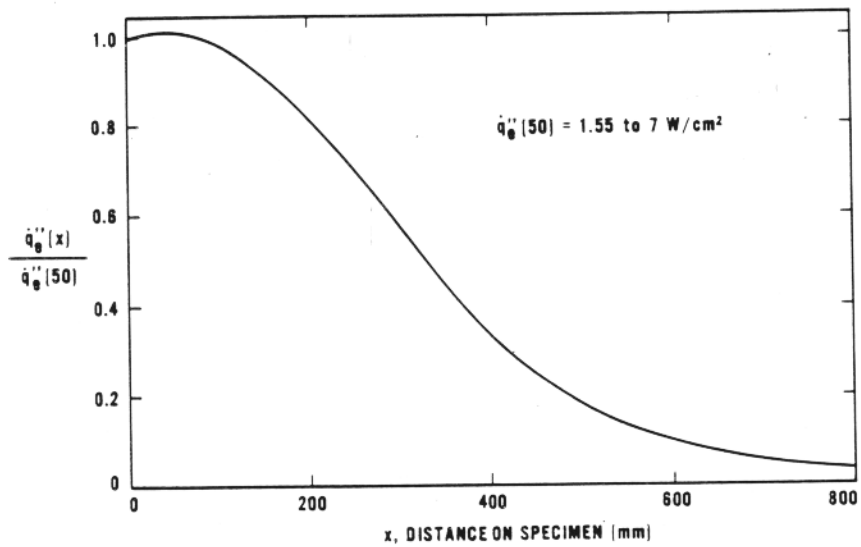


Figure 2. Normalized irradiance over the specimen.

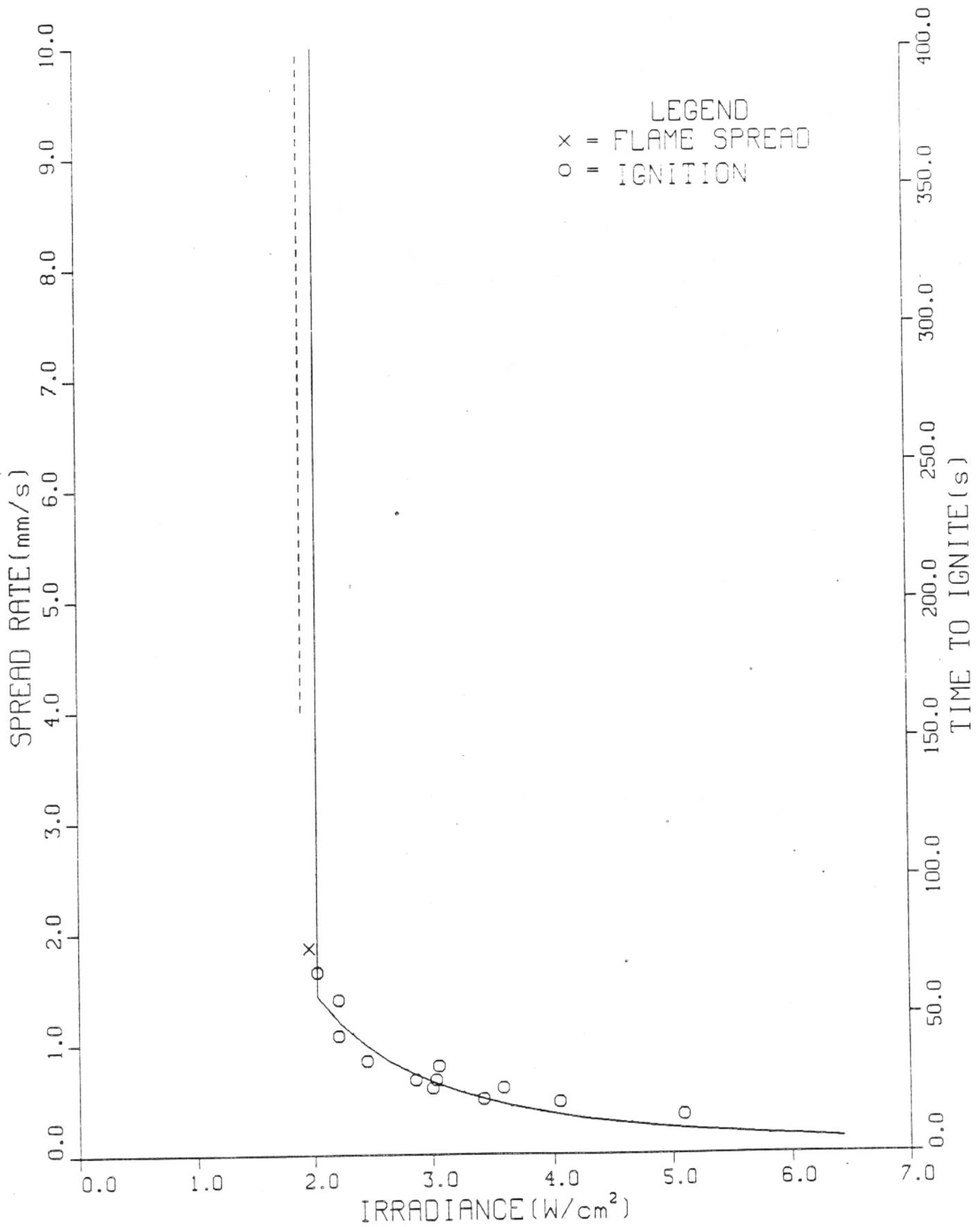


Figure-3. Correlation of ignition and flame spread results for the epoxy fiberglass panel.

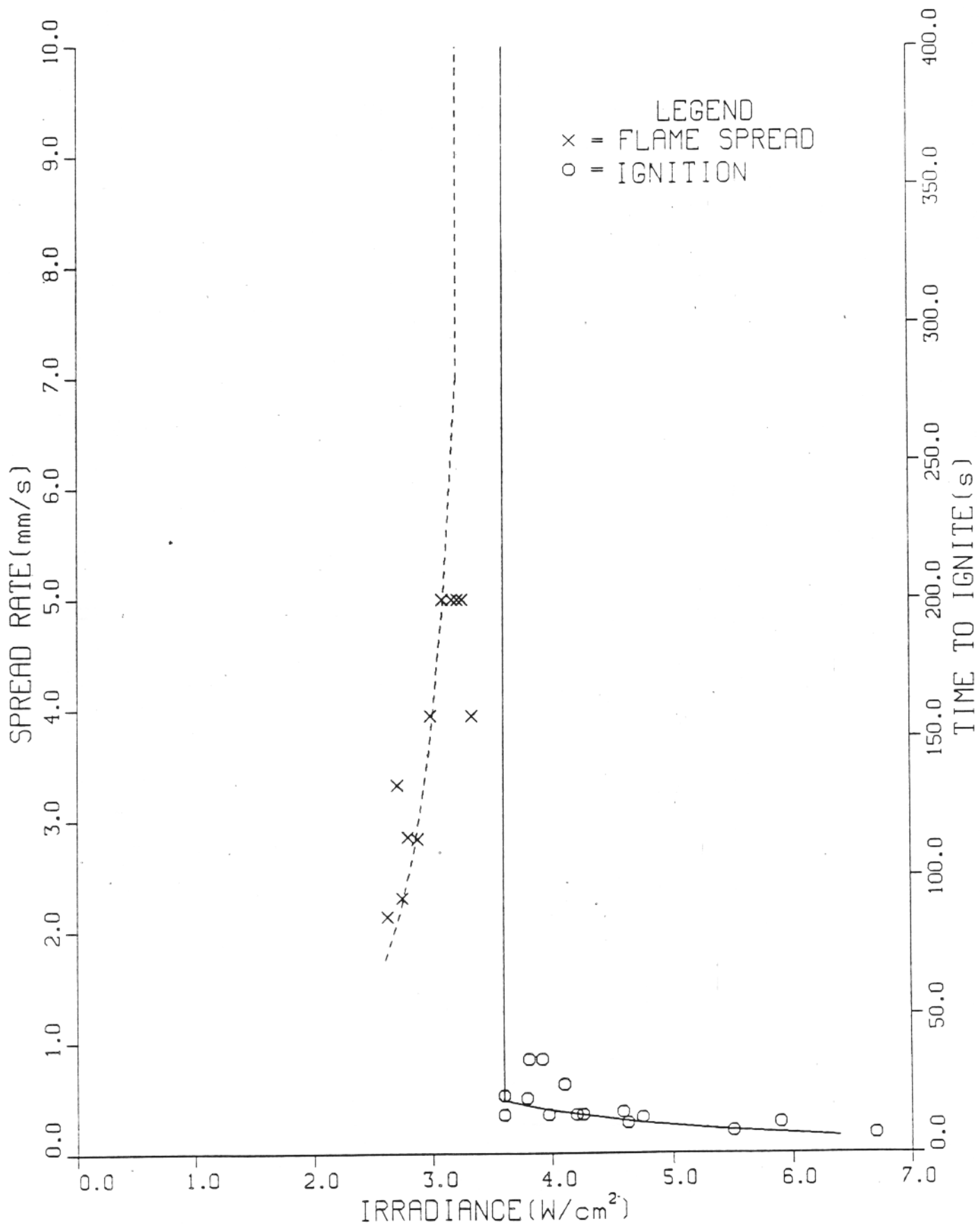


Figure 4. Correlation of ignition and flame spread results for the phenolic fiberglass panel.

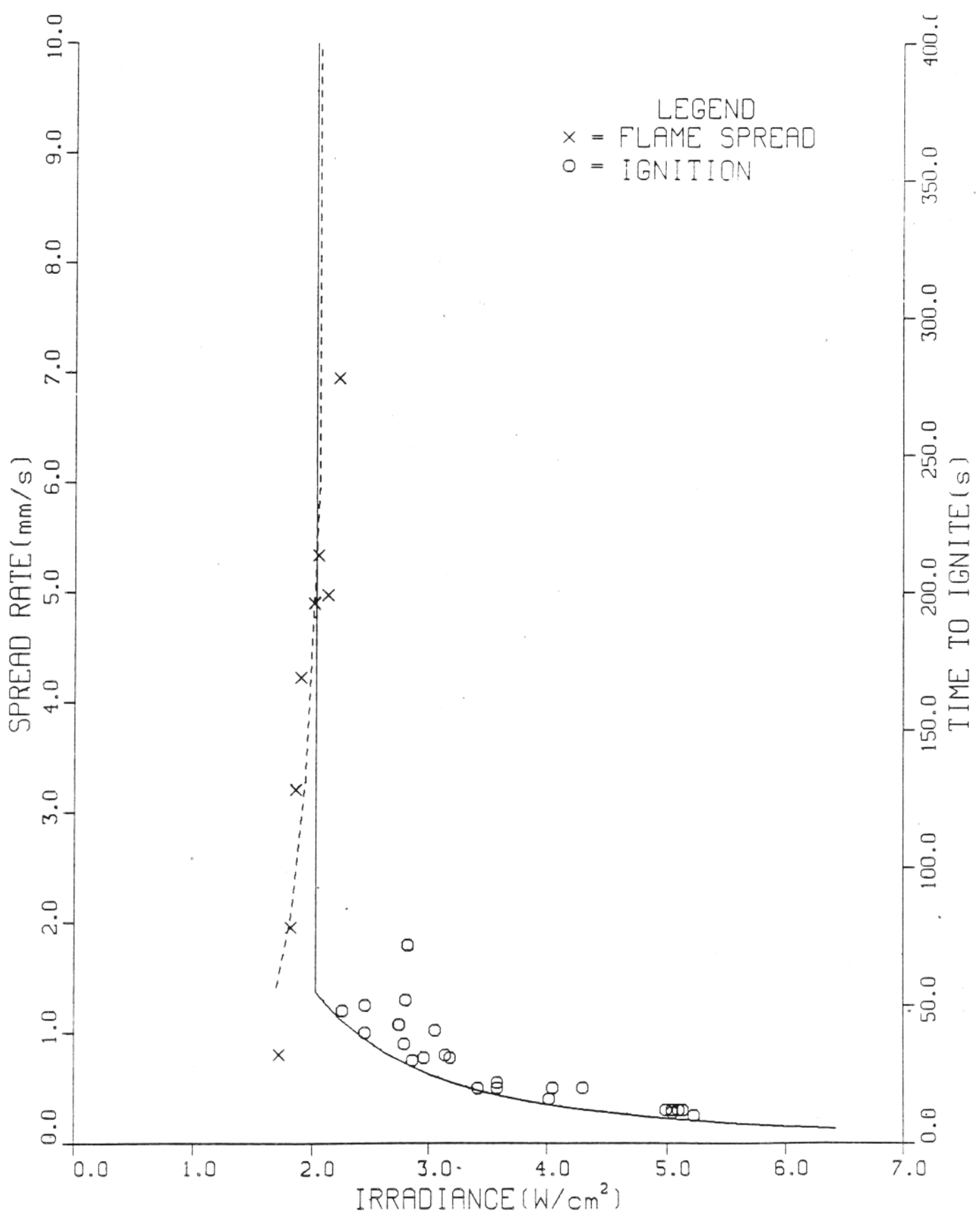


Figure 5. Correlation of ignition and flame spread results for the epoxy kevlar panel.

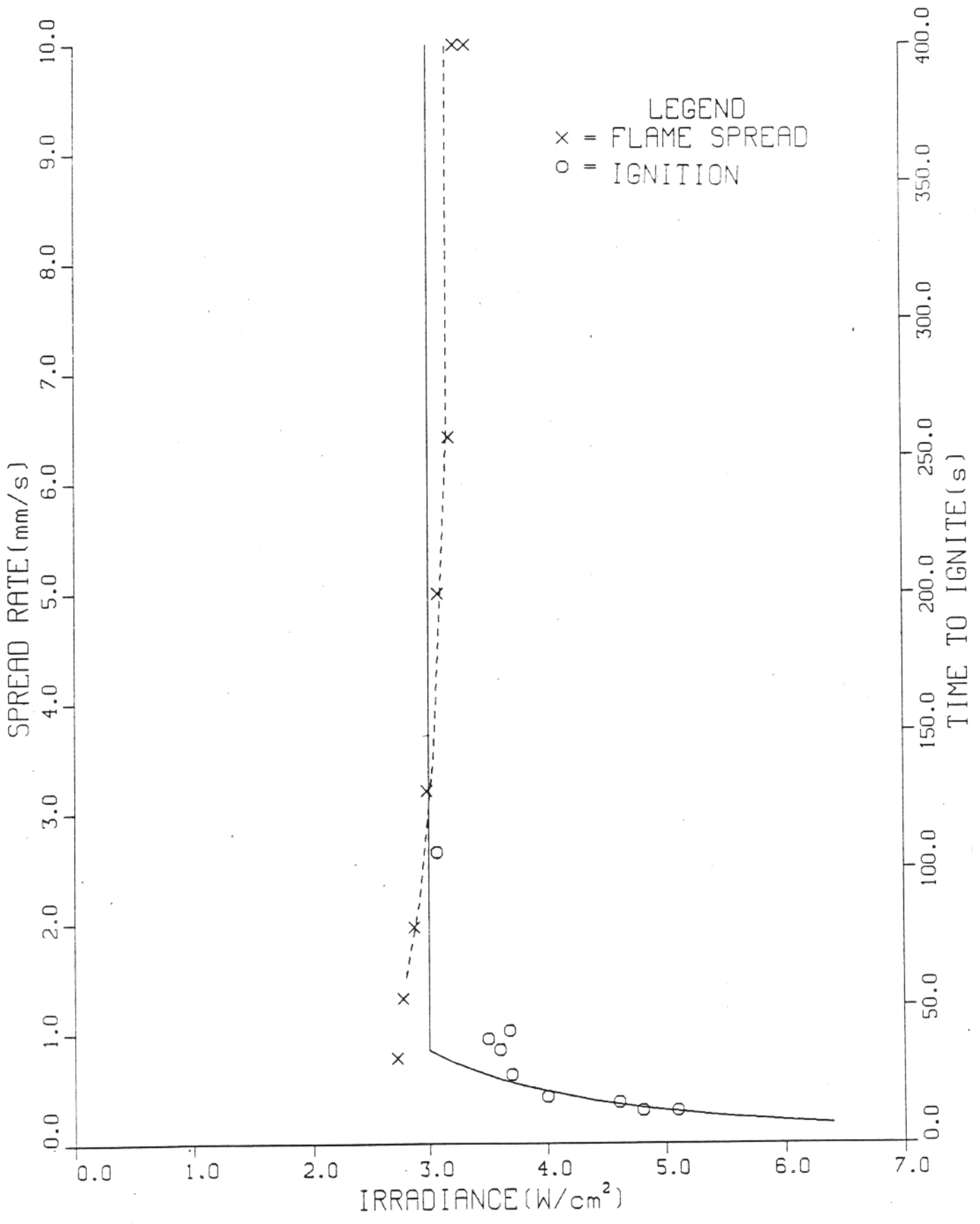


Figure 6. Correlation of ignition and flame spread results for the phenolic kevlar panel.

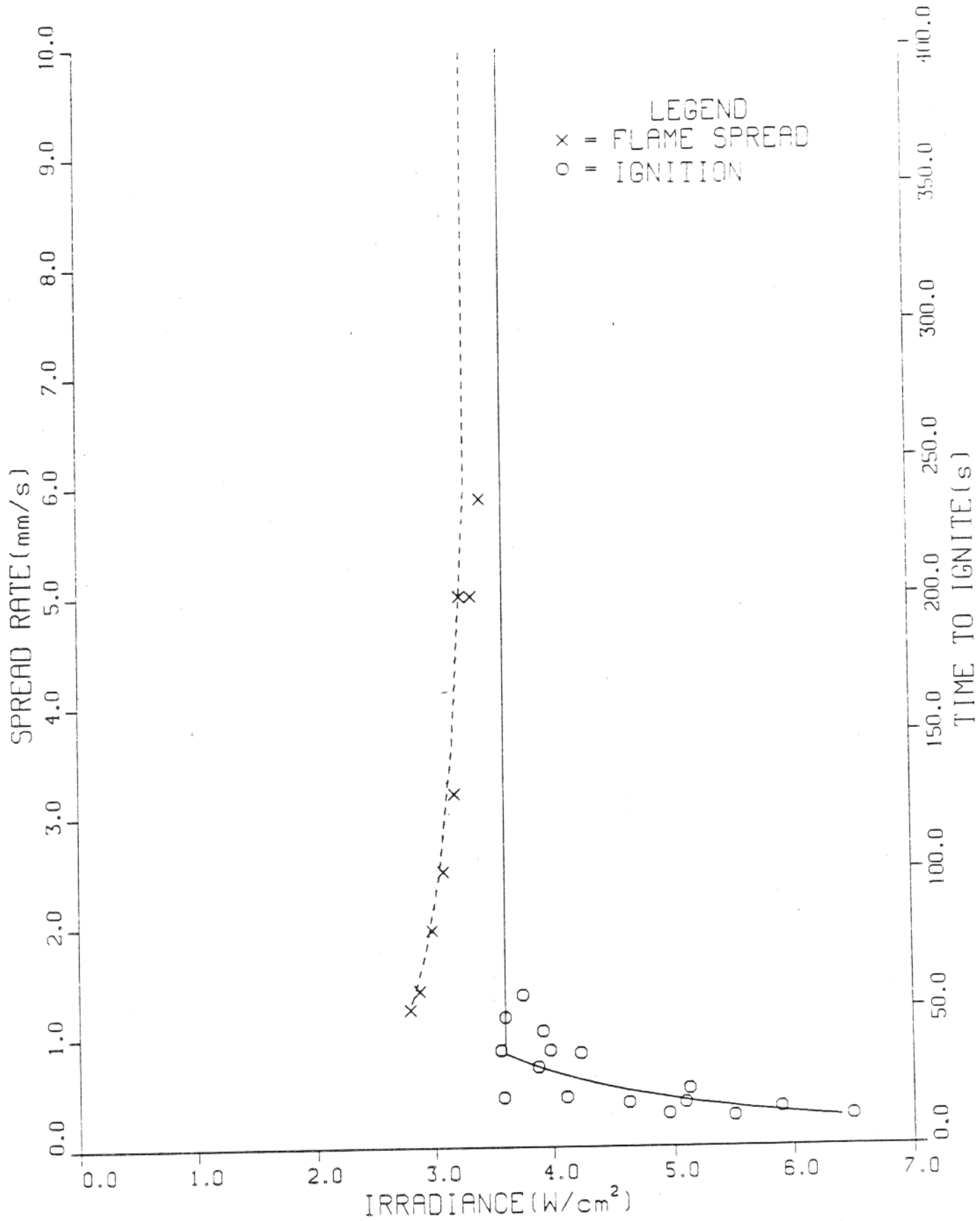


Figure 7. Correlation of ignition and flame spread results for the phenoloc graphite panel.

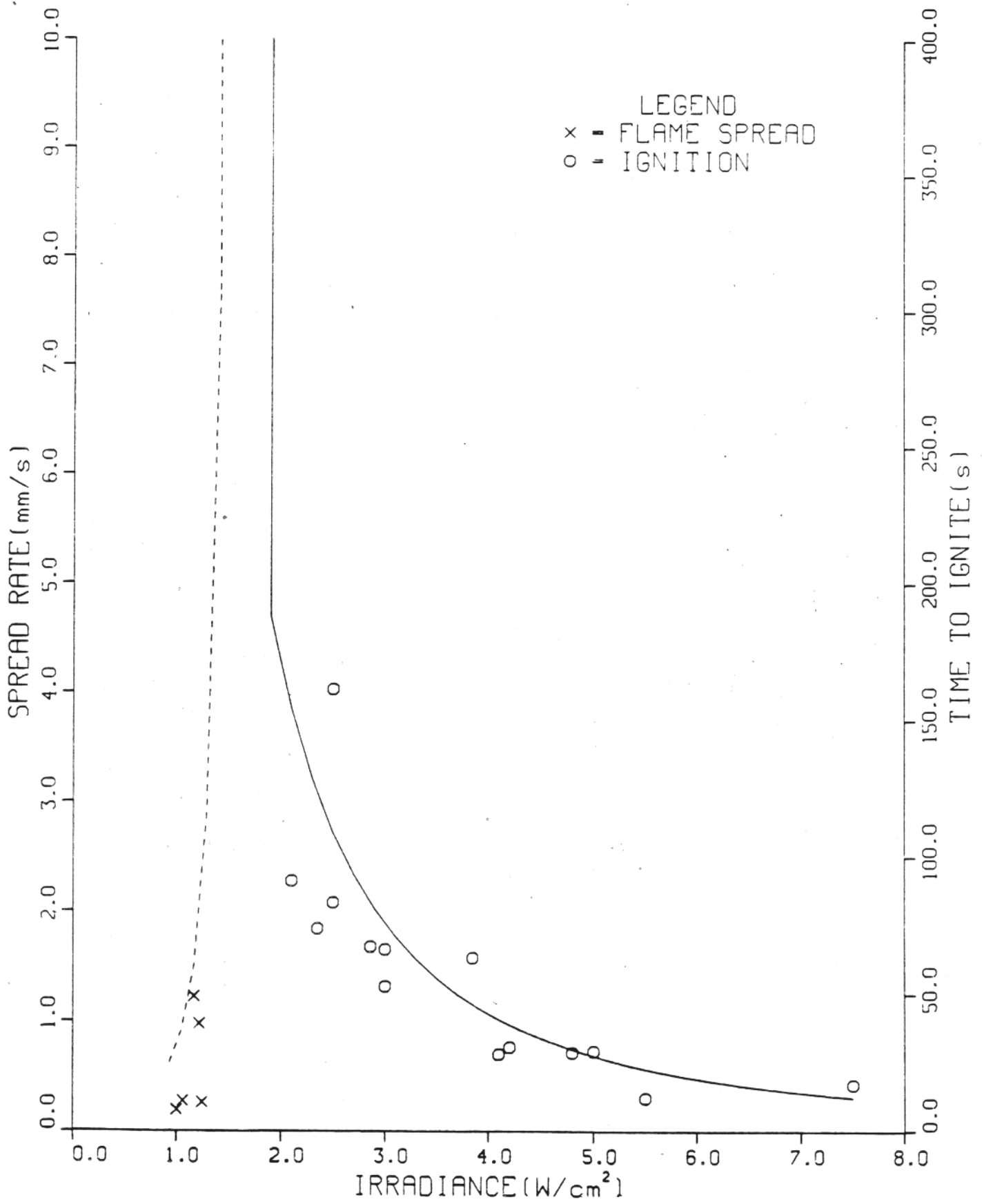


Figure 8. Correlation of ignition and flame spread results for the ABS panel.

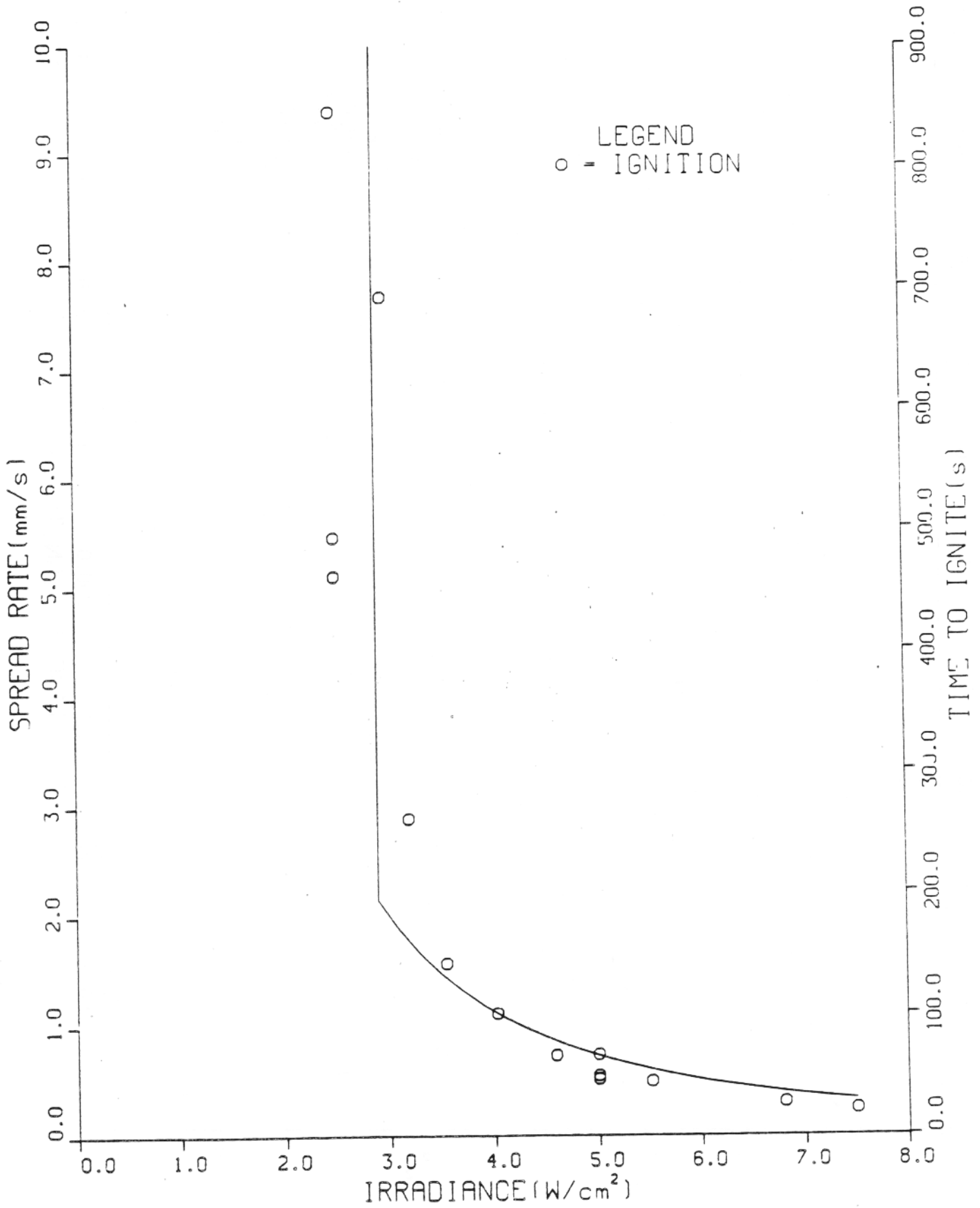


Figure 9. Correlation of ignition and flame spread results for the polycarbonate panel.

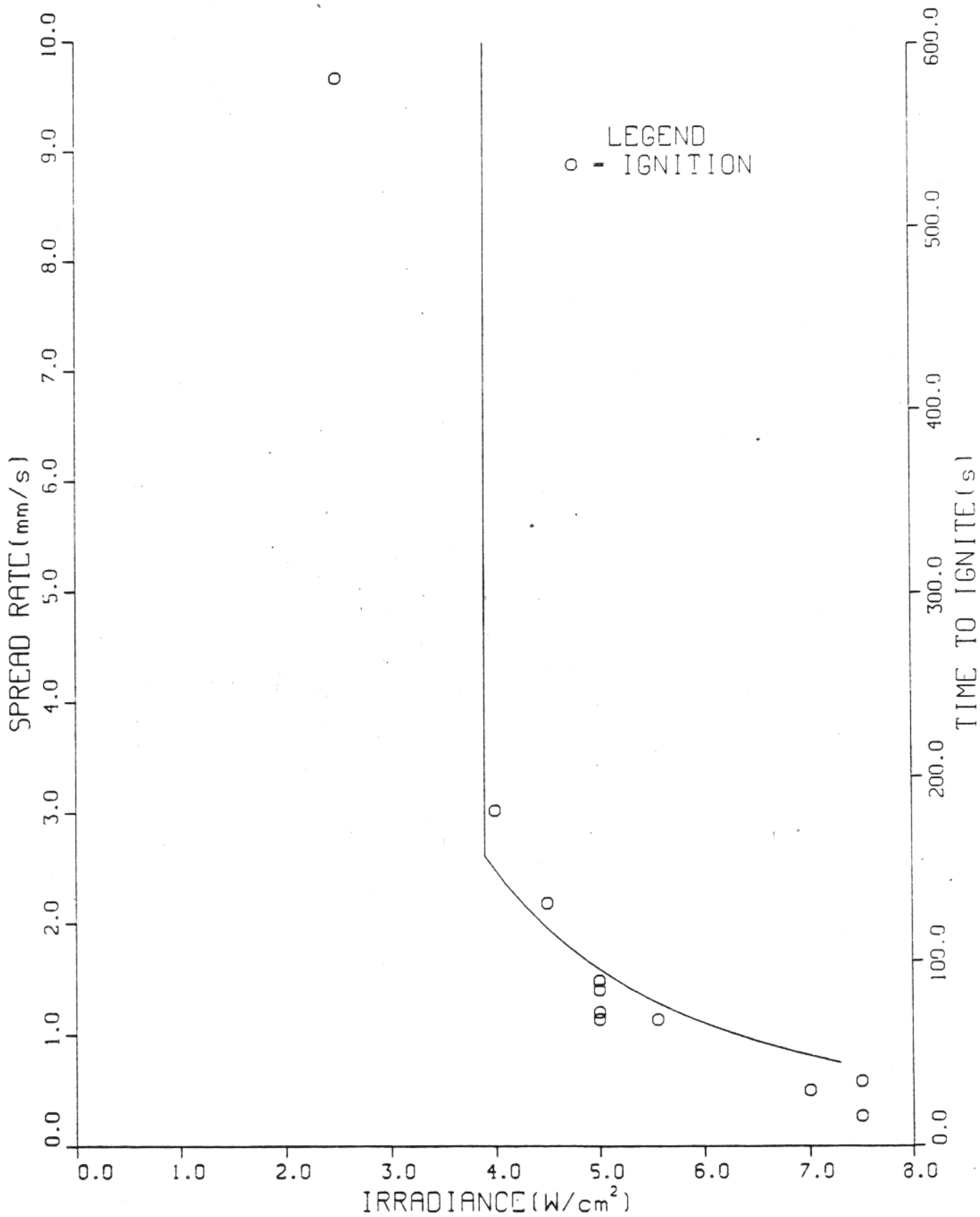


Figure 10. Correlation of ignition and flame spread results for the ULTEM panel.

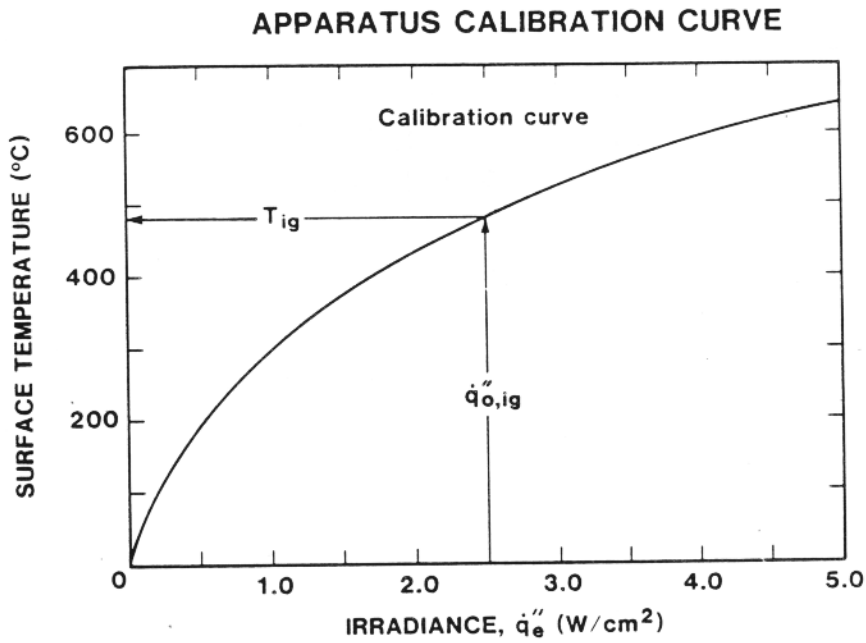


Figure 11. Equilibrium surface temperatures as a function of external radiant heating in the test apparatus.

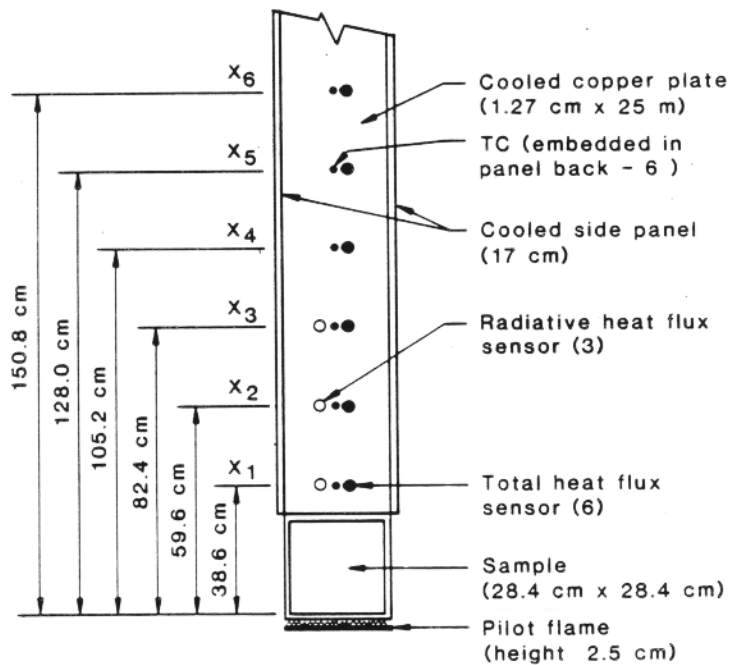


Figure 12. Schematic of heat transfer apparatus.

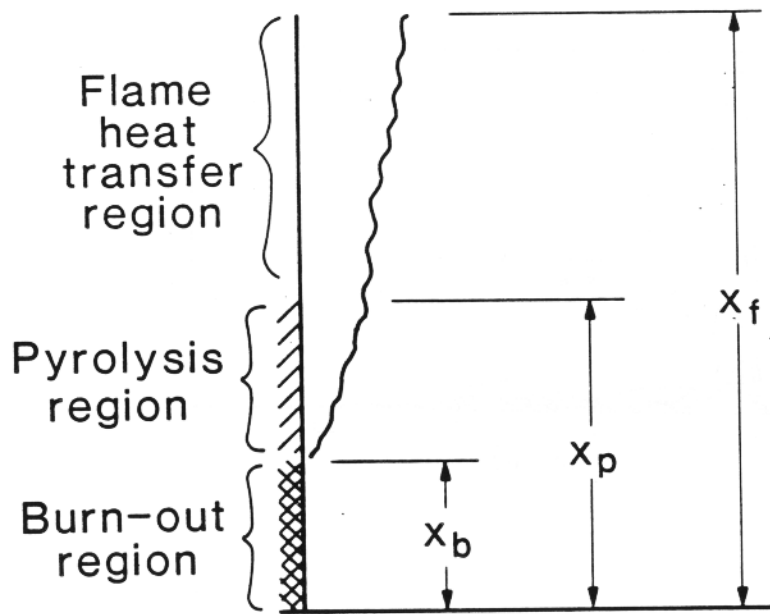


Figure 13. Flame spread problem.

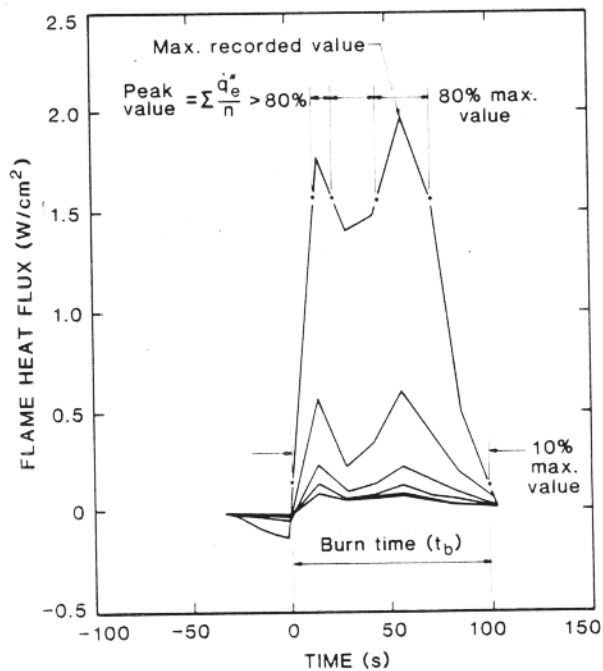


Figure 14. Procedure for determining average peak burning values.

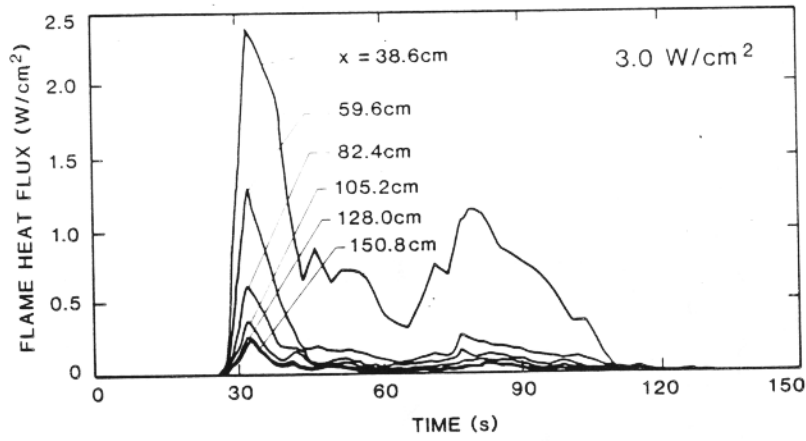


Figure 15-A. Flame heat transfer to vertical wall above panel with epoxy/fiberglass facing.

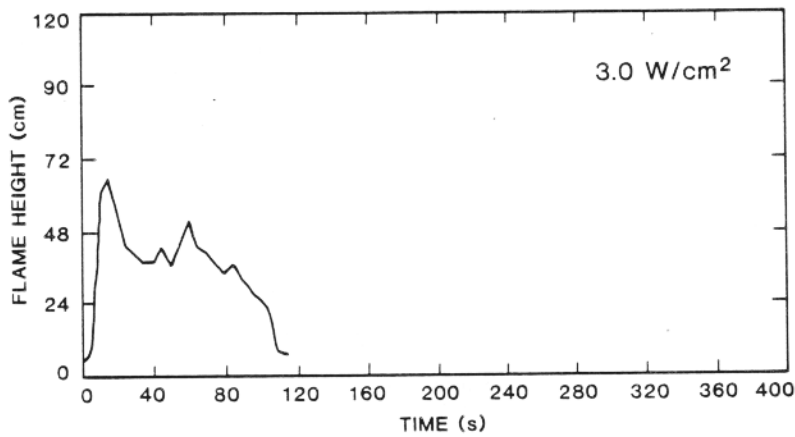


Figure 15-B. Flame height from base of burning panel with epoxy/fiberglass facing.

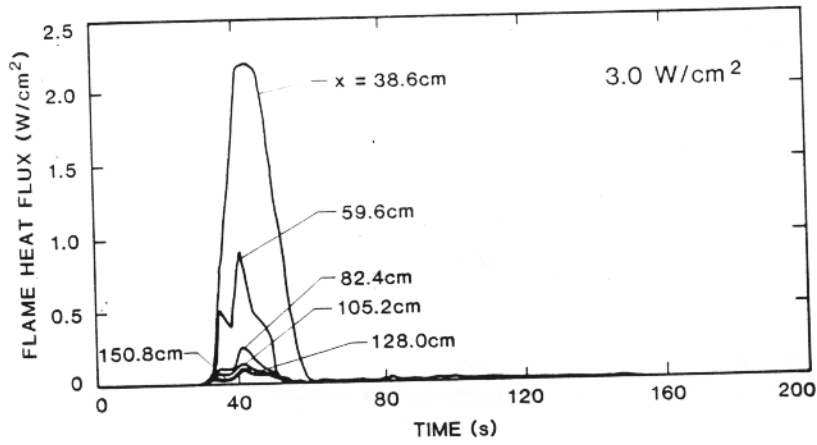


Figure 16-A. Flame heat transfer to vertical wall above panel with phenolic/fiberglass facing.

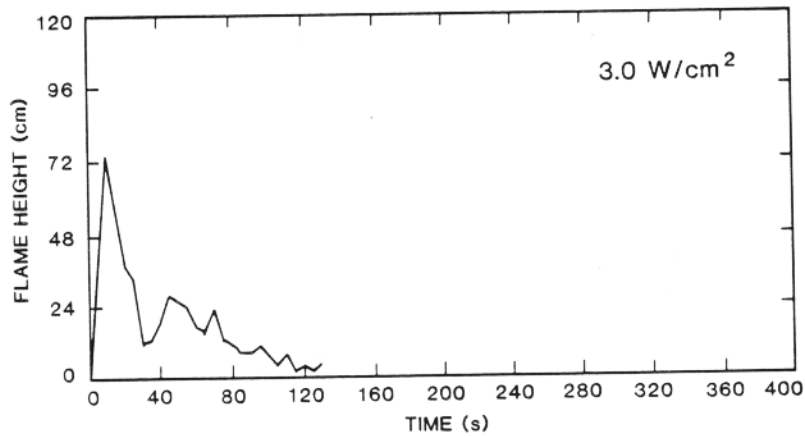


Figure 16-B. Flame height from base of burning panel with phenolic/fiberglass facing.

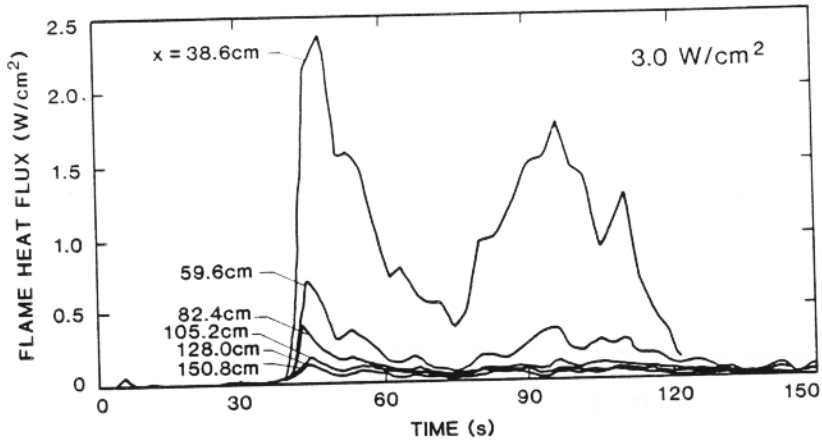


Figure 17-A. Flame heat transfer to vertical wall above panel with epoxy/kevlar facing.

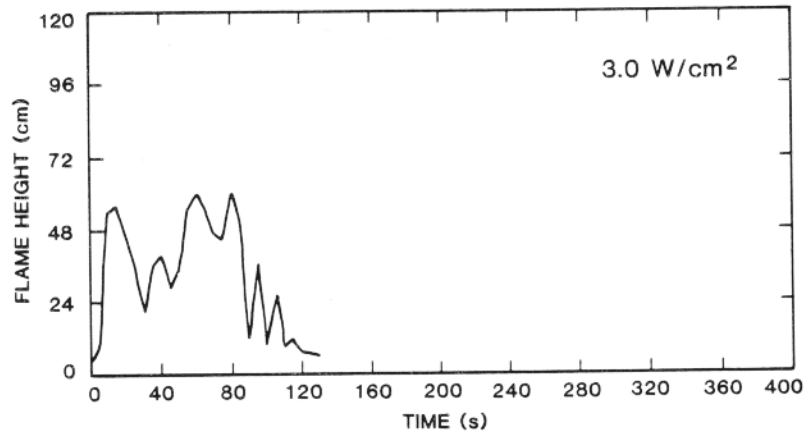


Figure 17-B. Flame height from base of burning panel with epoxy/kevlar facing.

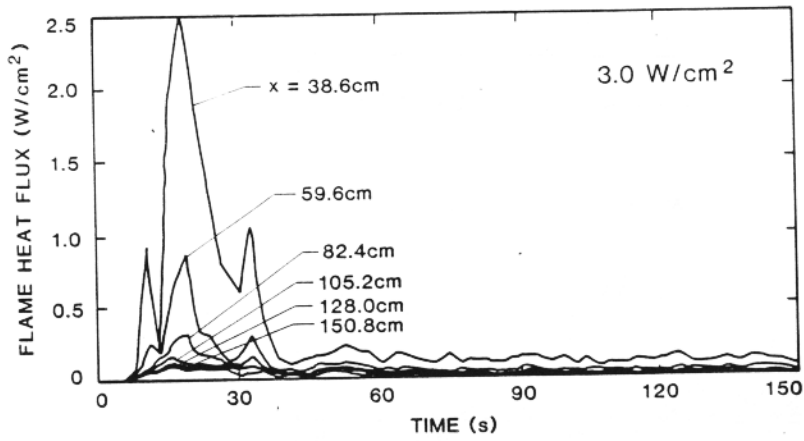


Figure 18-A. Flame heat transfer to vertical wall above panel with phenolic/kevlar facing.

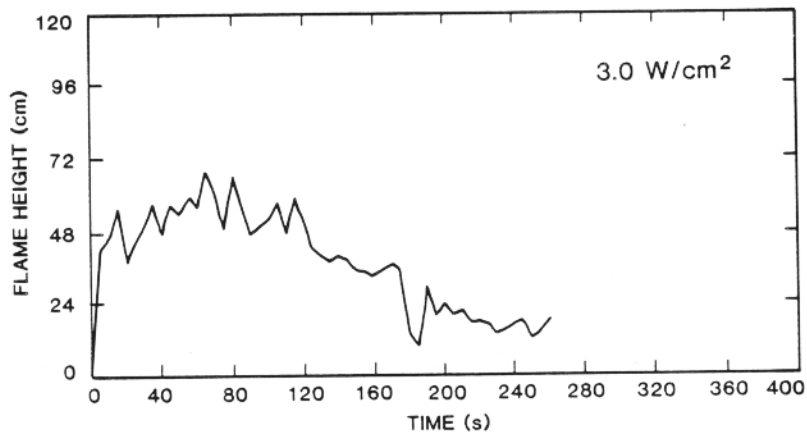


Figure 18-B. Flame height from base of burning panel with phenolic/kevlar facing.

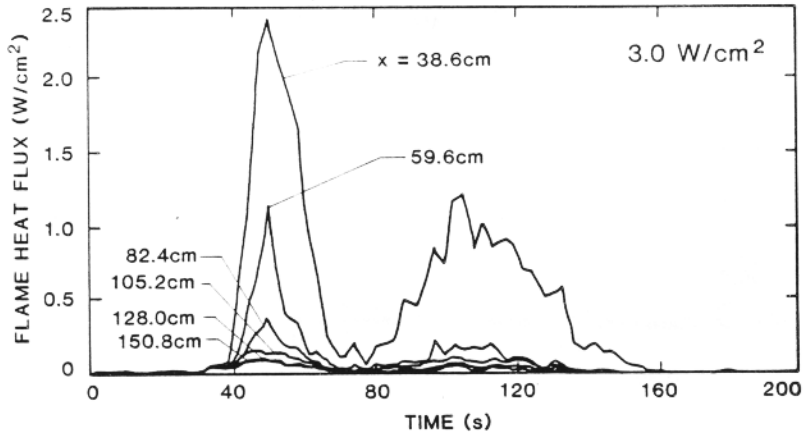


Figure 19-A. Flame heat transfer to vertical wall above panel with phenolic/graphite facing.

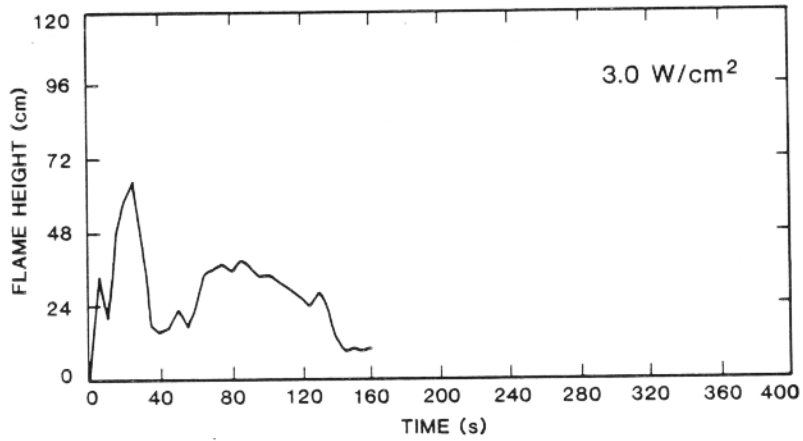


Figure 19-B. Flame height from base of burning panel with phenolic/graphite facing.

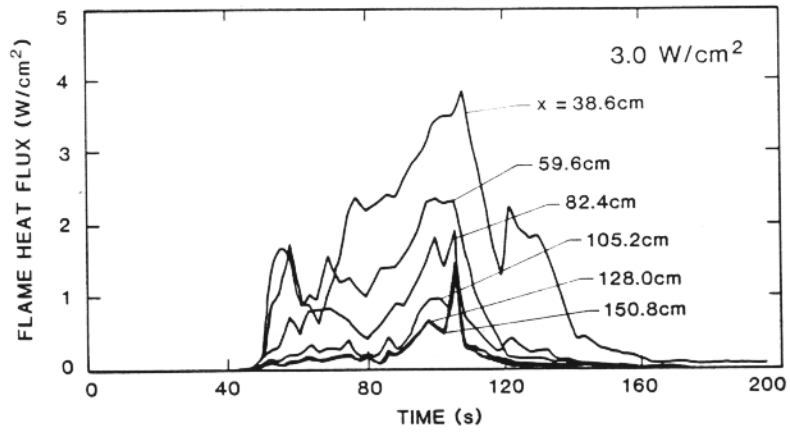


Figure 20-A. Flame heat transfer to vertical wall above ABS panel.

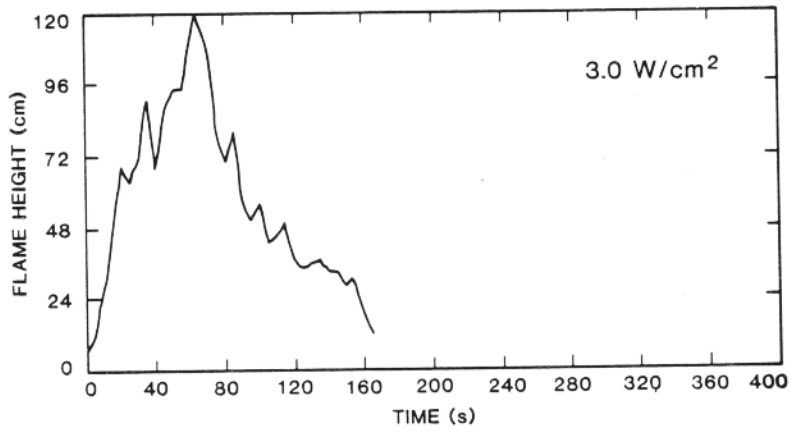


Figure 20-B. Flame height from base of burning ABS panel.

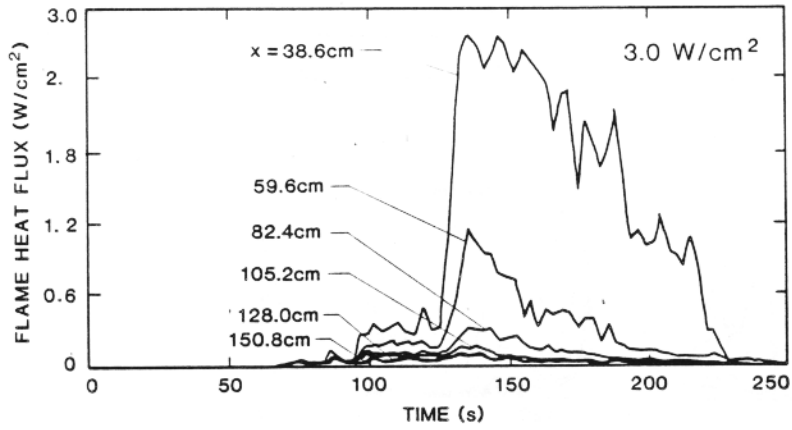


Figure 21-A. Flame heat transfer to vertical wall above polycarbonate panel.

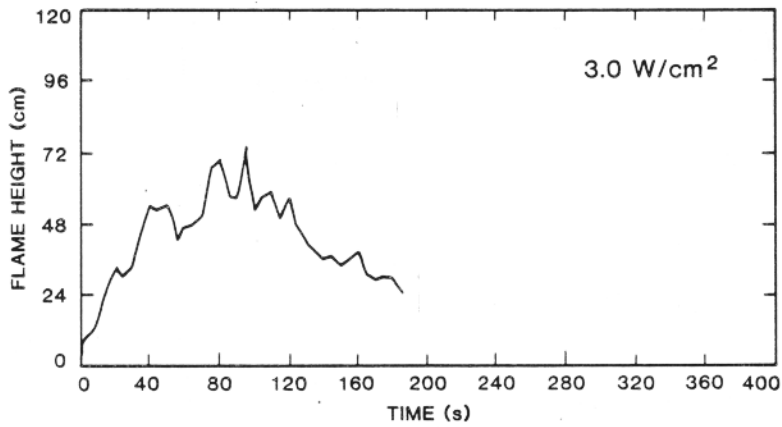


Figure 21-B. Flame height from base of burning polycarbonate panel.

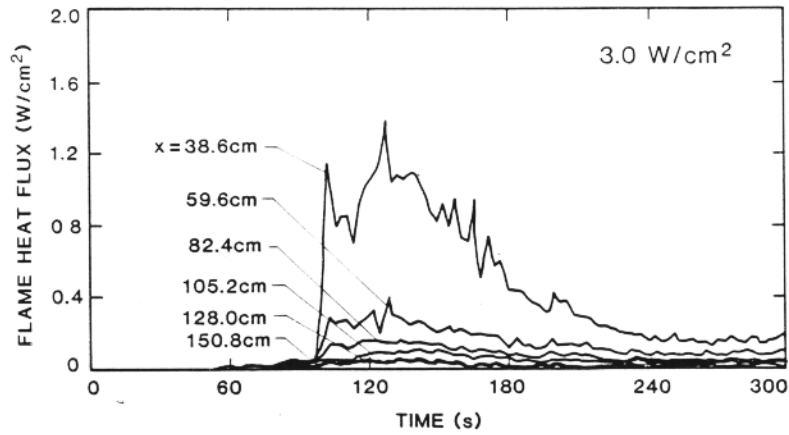


Figure 22-A. Flame heat transfer to vertical wall above ULTEM panel.

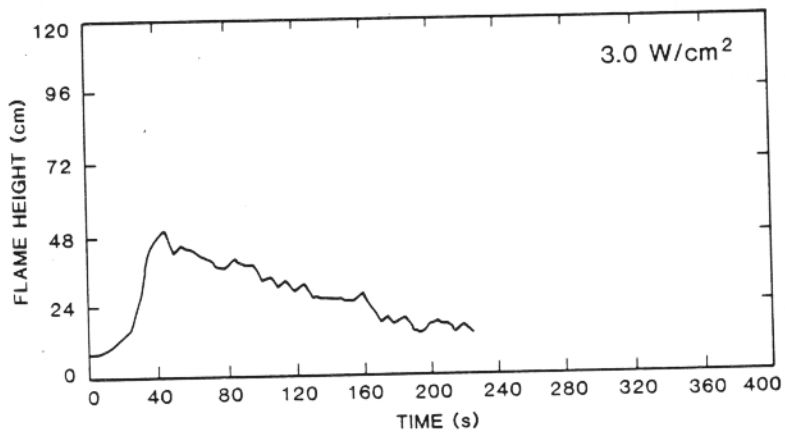


Figure 22-B. Flame height from base of burning ULTEM panel.

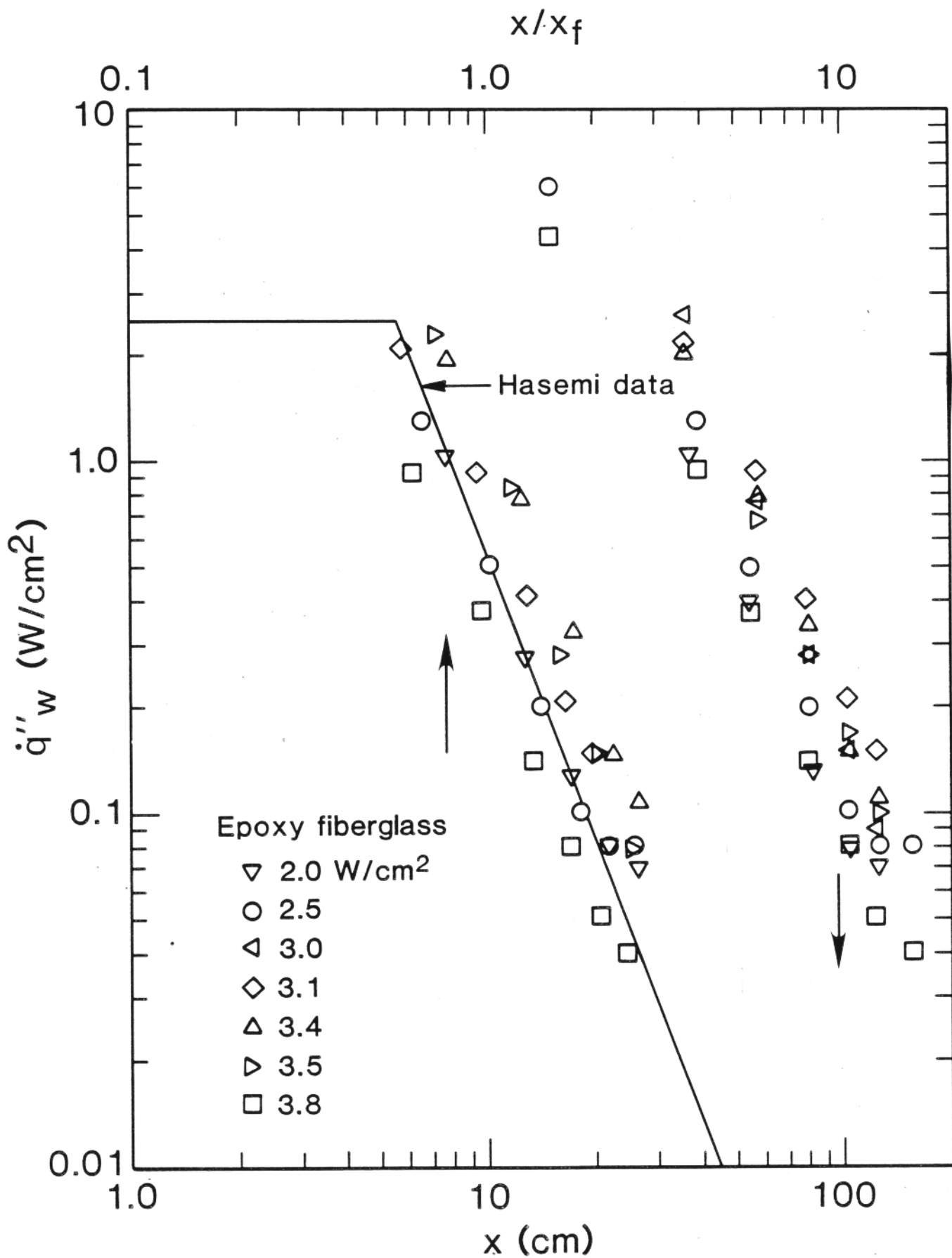


Figure 23. Wall heat flux distribution for epoxy/fiberglass panel.

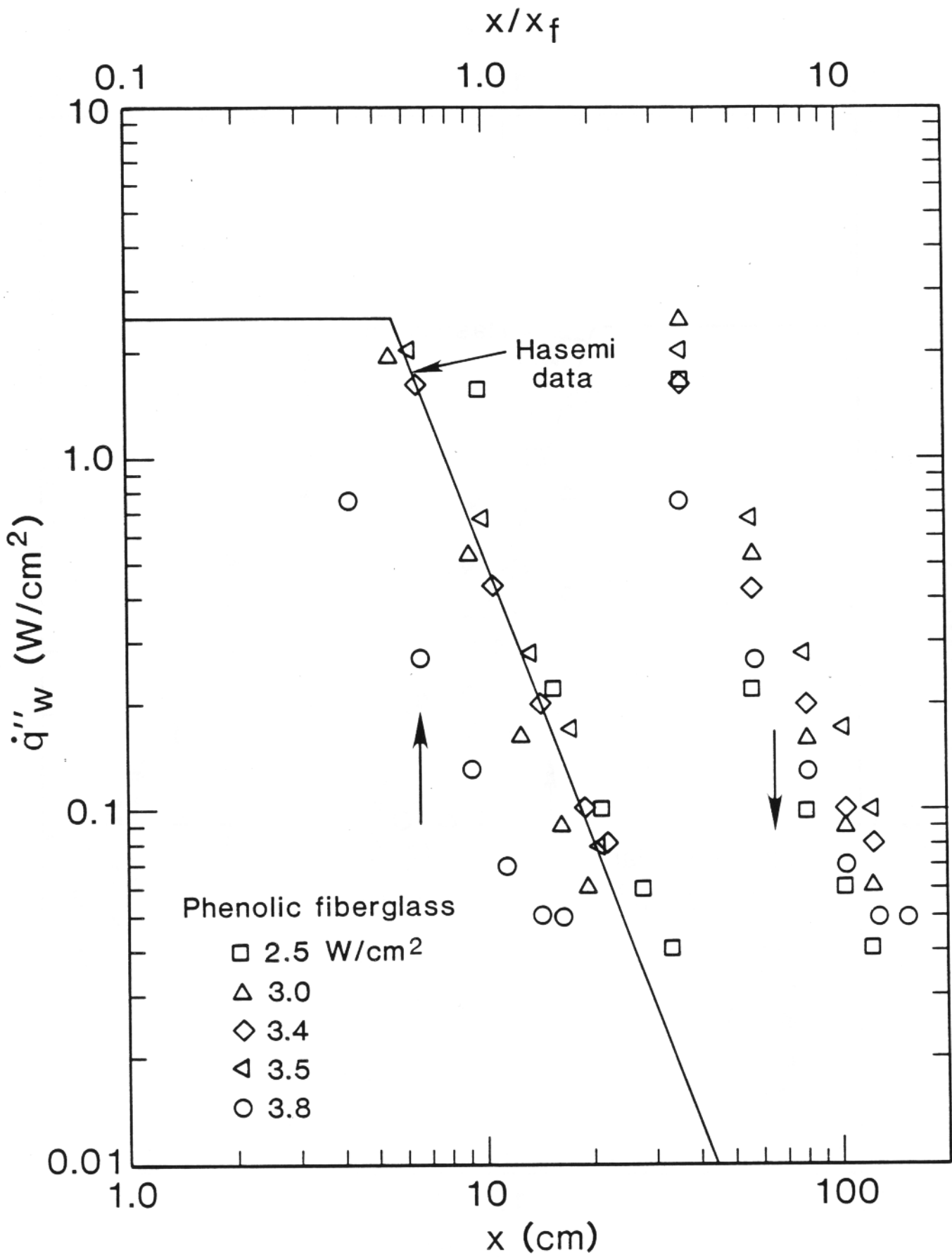


Figure 24. Wall heat flux distribution for phenolic/fiberglass panel.

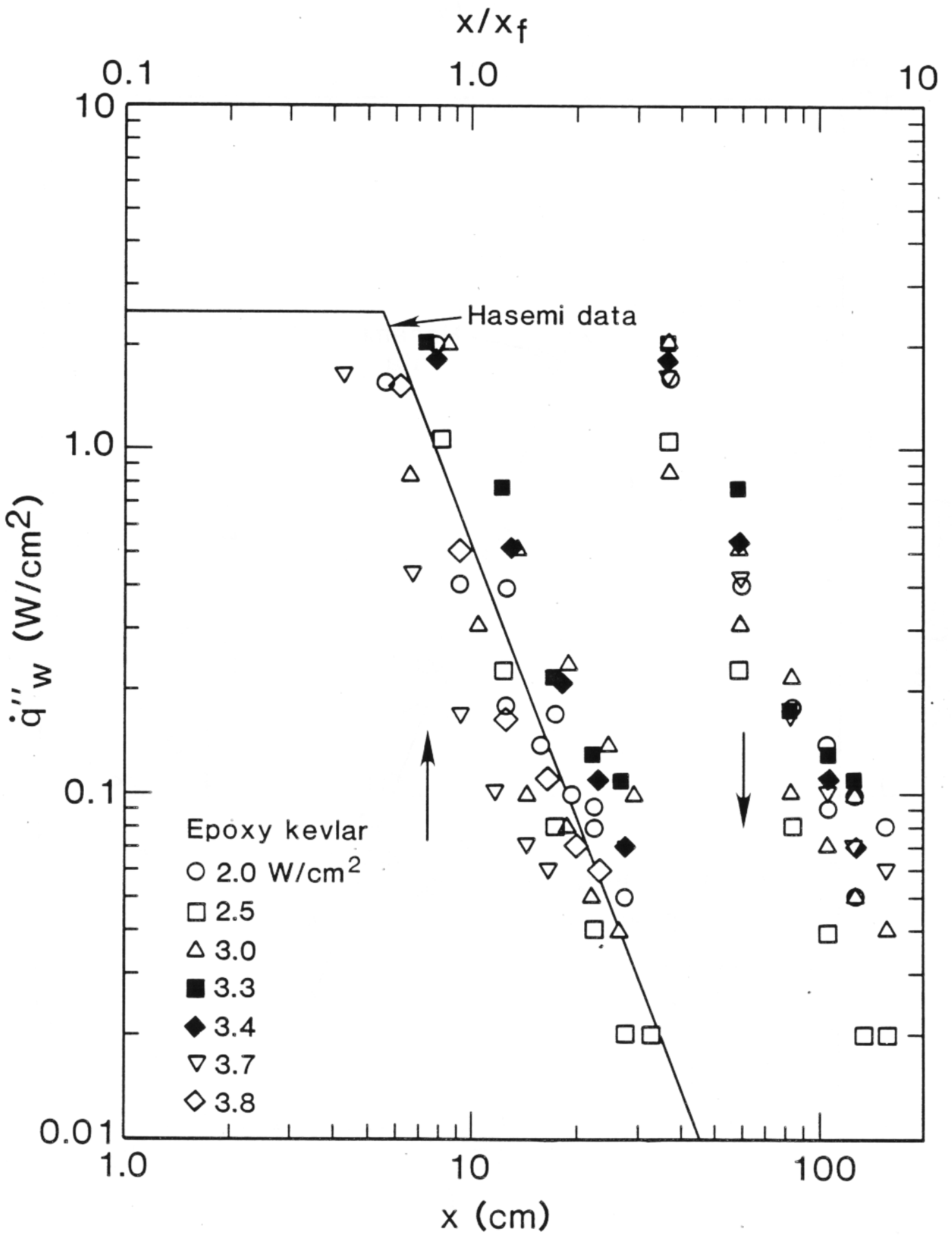


Figure 25. Wall heat flux distribution for epoxy/kevlar panel.

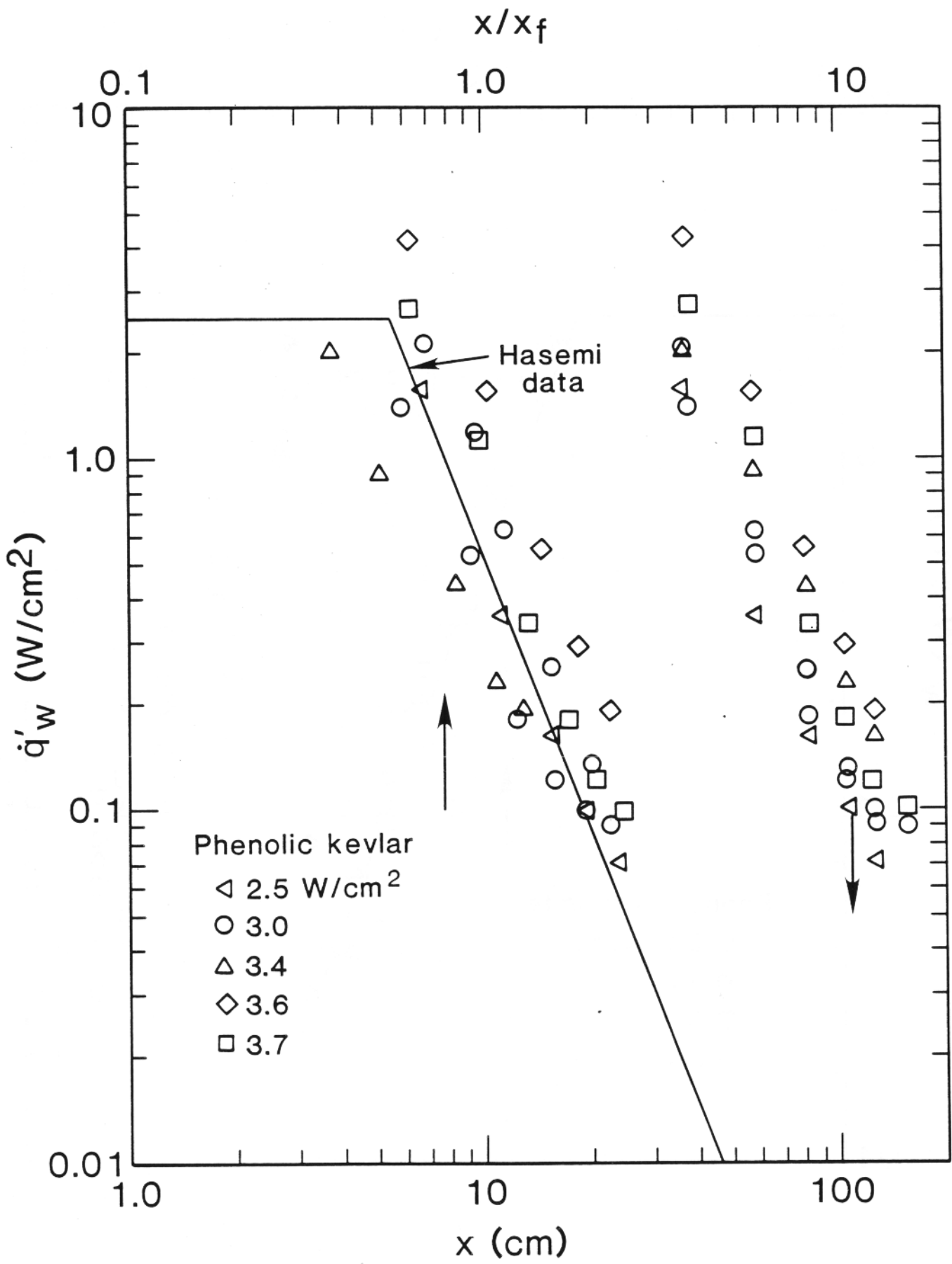


Figure 26. Wall heat flux distribution for phenolic/kevlar panel.

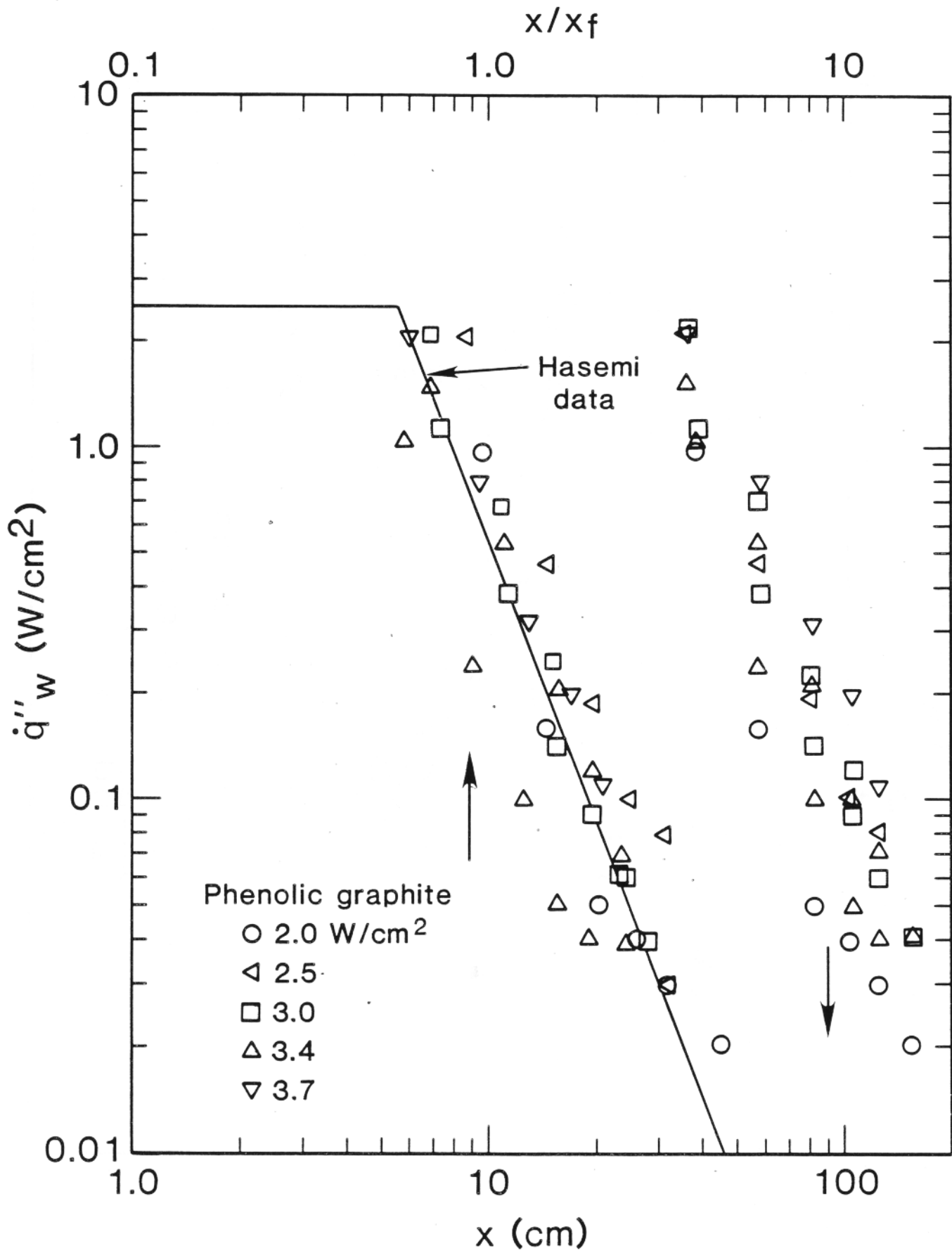


Figure 27. Wall heat flux distribution for phenolic/graphite panel.

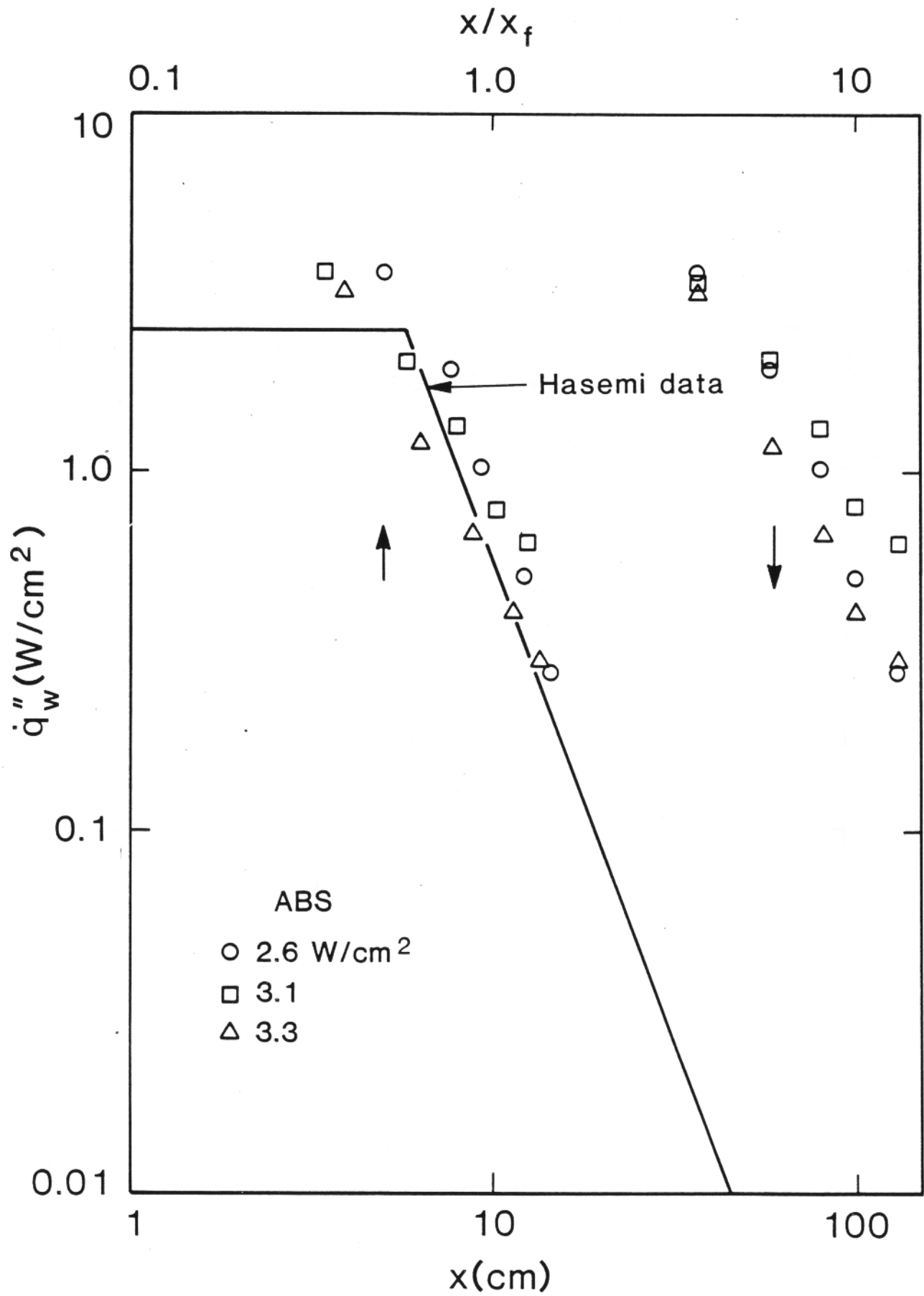


Figure 28. Wall heat flux distribution for ABS panel.

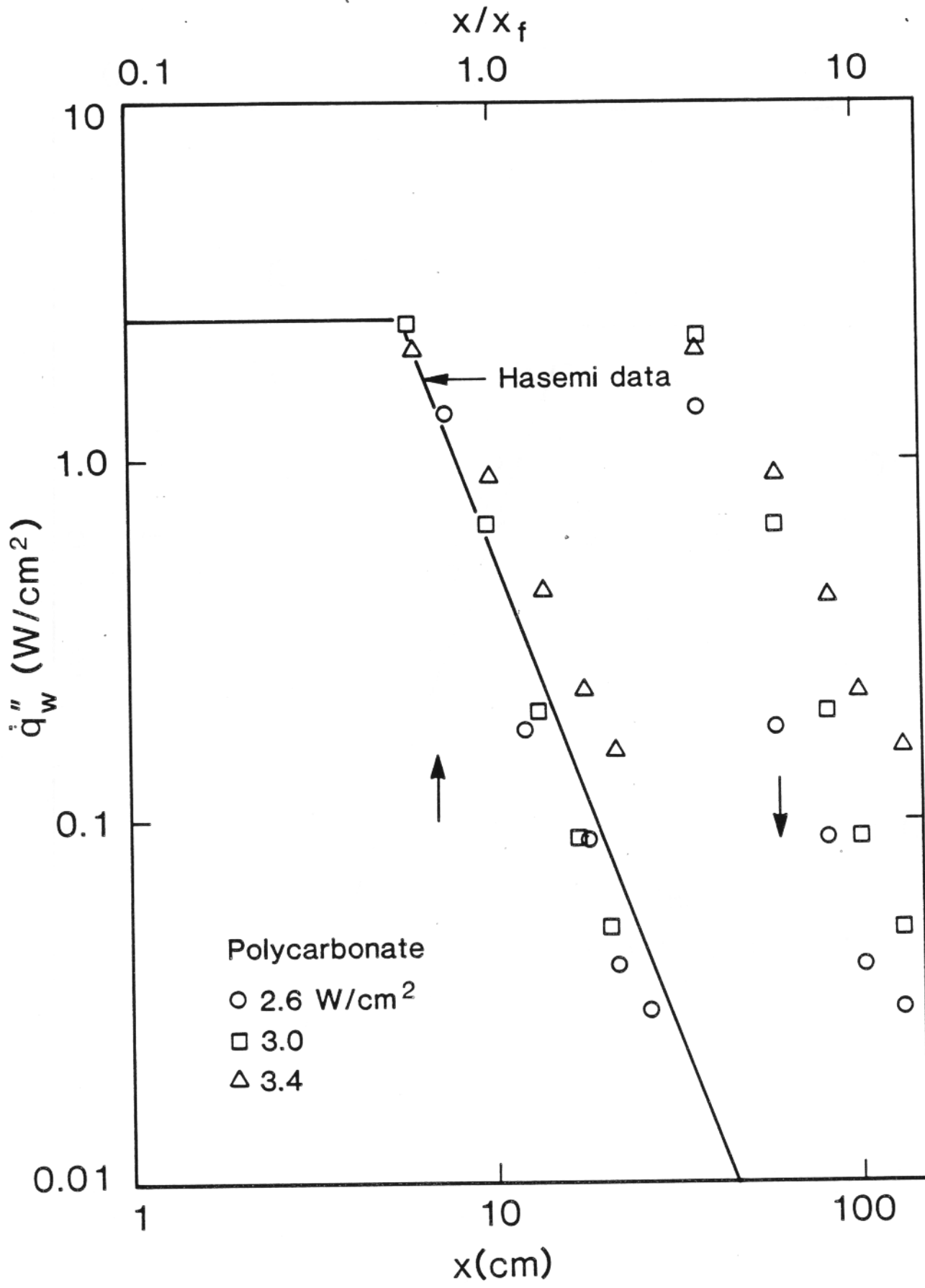


Figure 29. Wall heat flux distribution for polycarbonate panel.

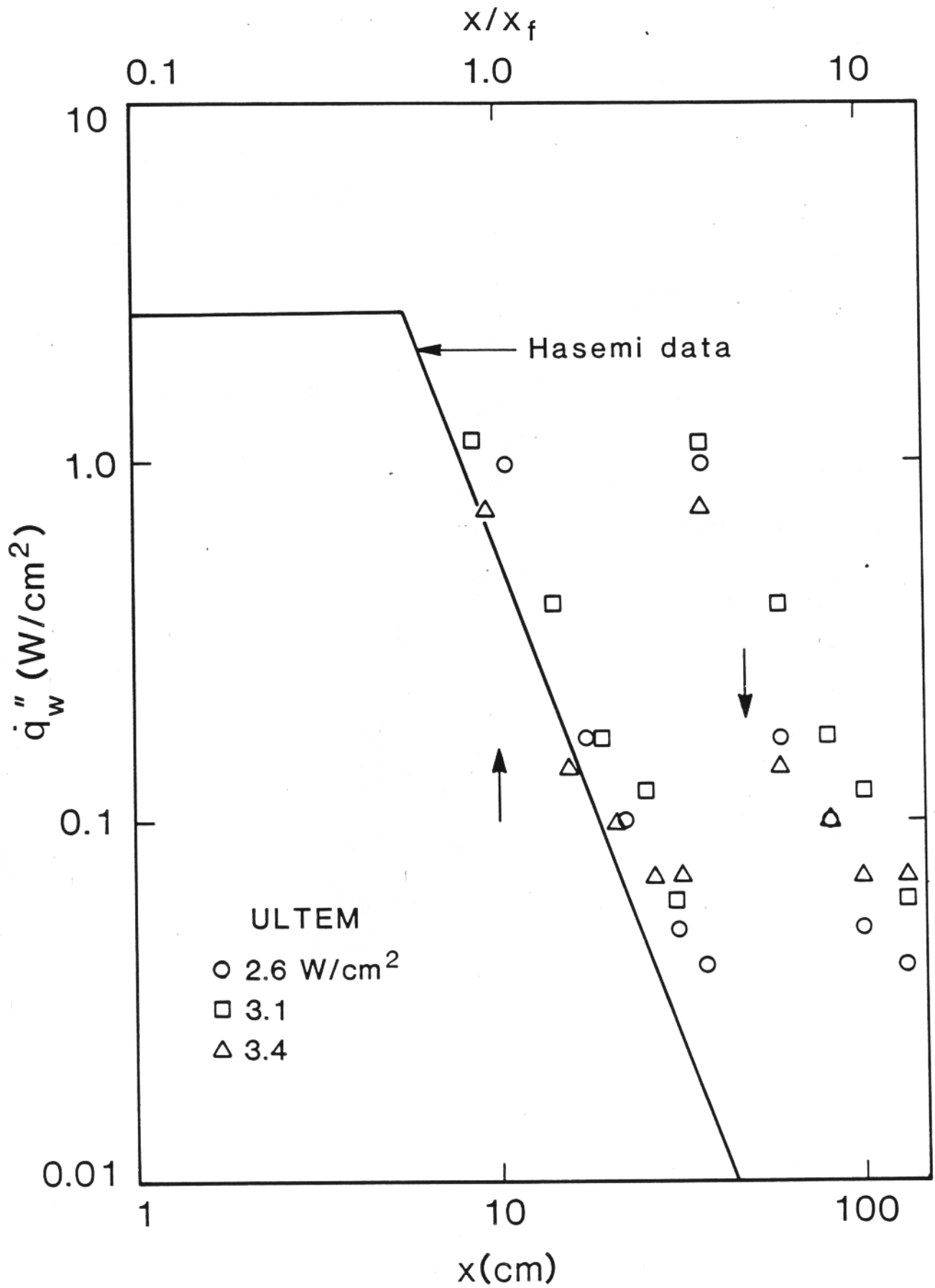


Figure 30. Wall heat flux distribution for ULTEM panel.

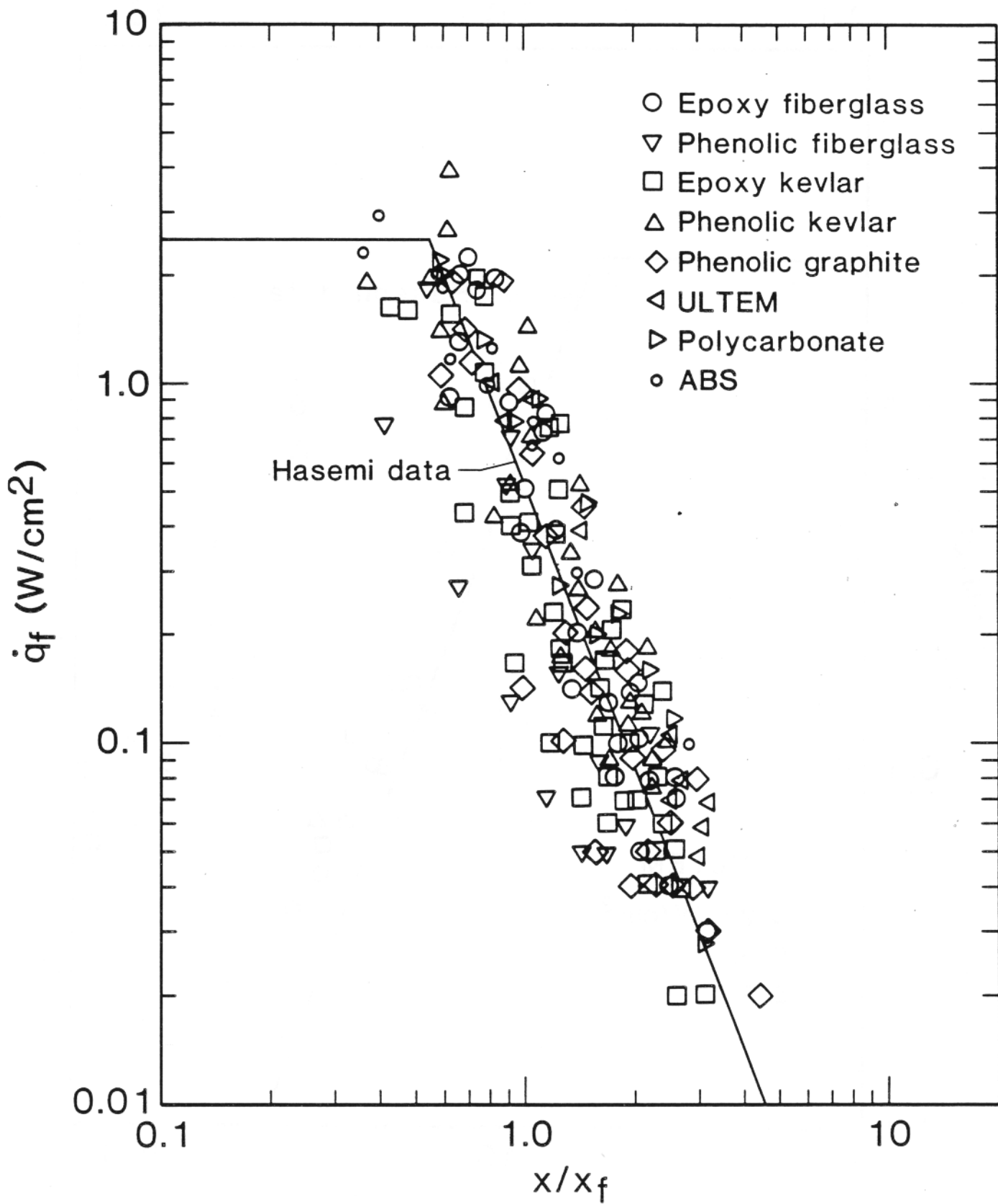


Figure 31. Wall heat flux in terms of x/x_f .

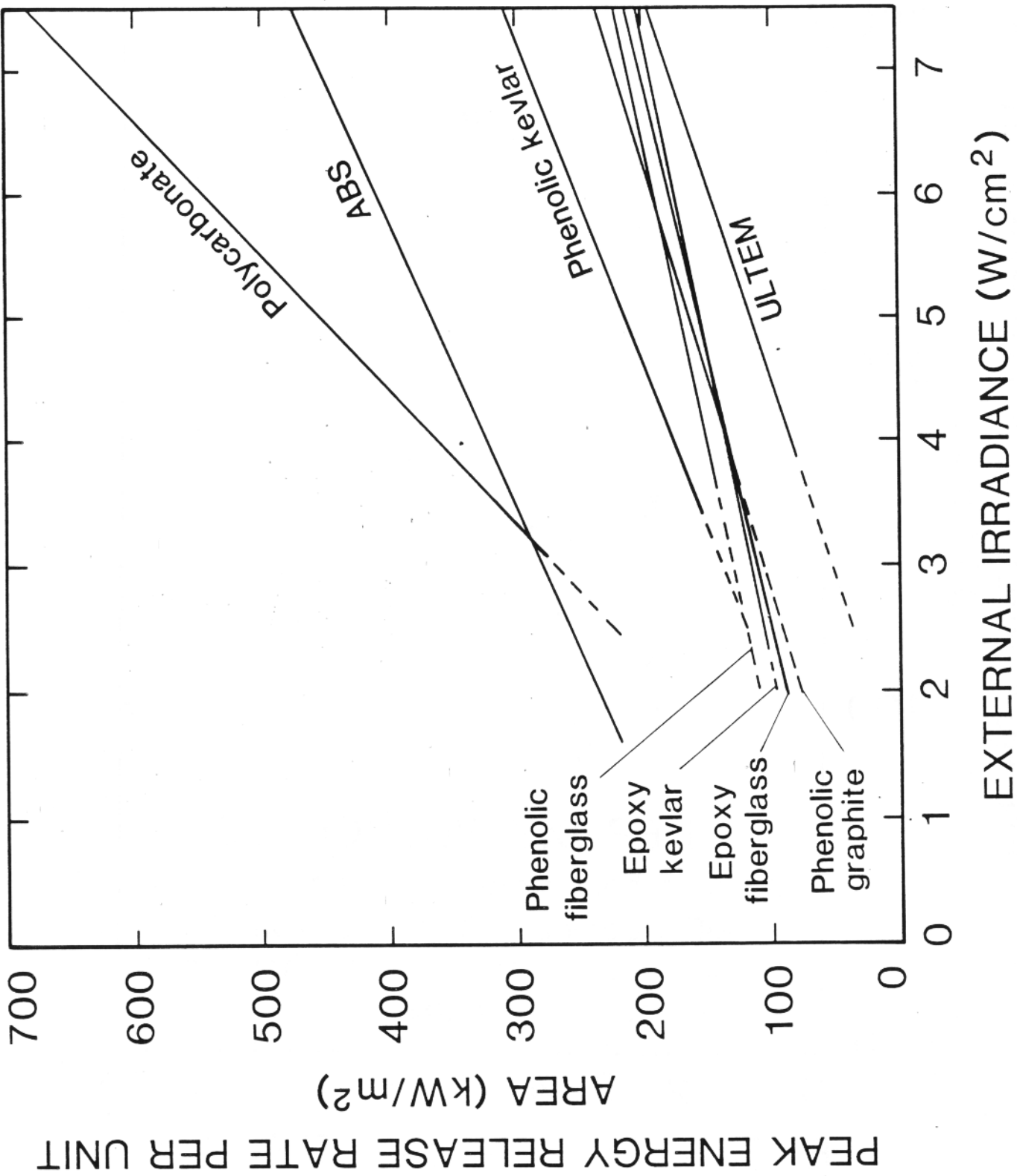


Figure 32. Peak energy release rate under external irradiance.

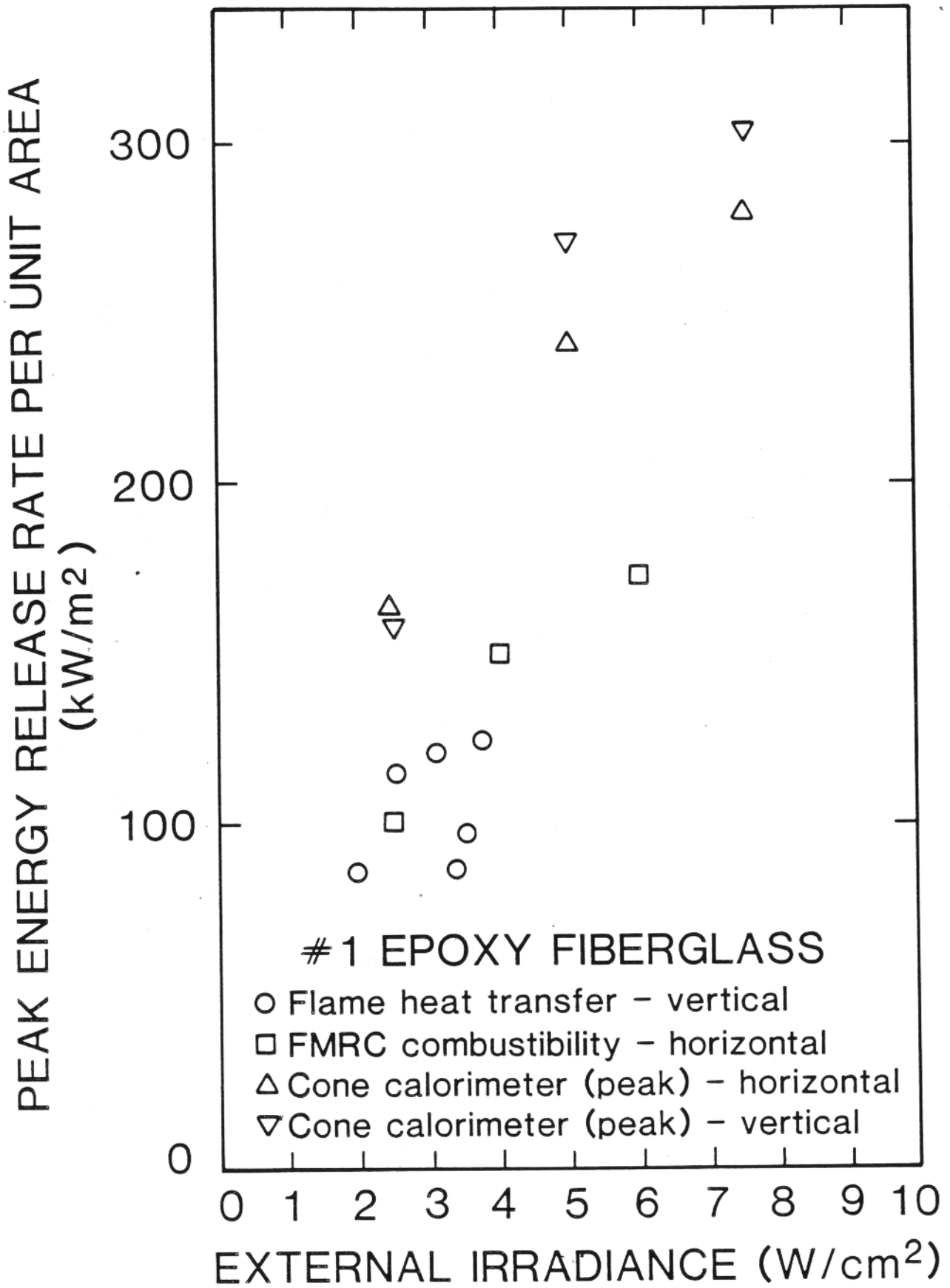


Figure 33. Peak energy release rate for epoxy/fiberglass panel.

PEAK ENERGY RELEASE RATE PER UNIT AREA

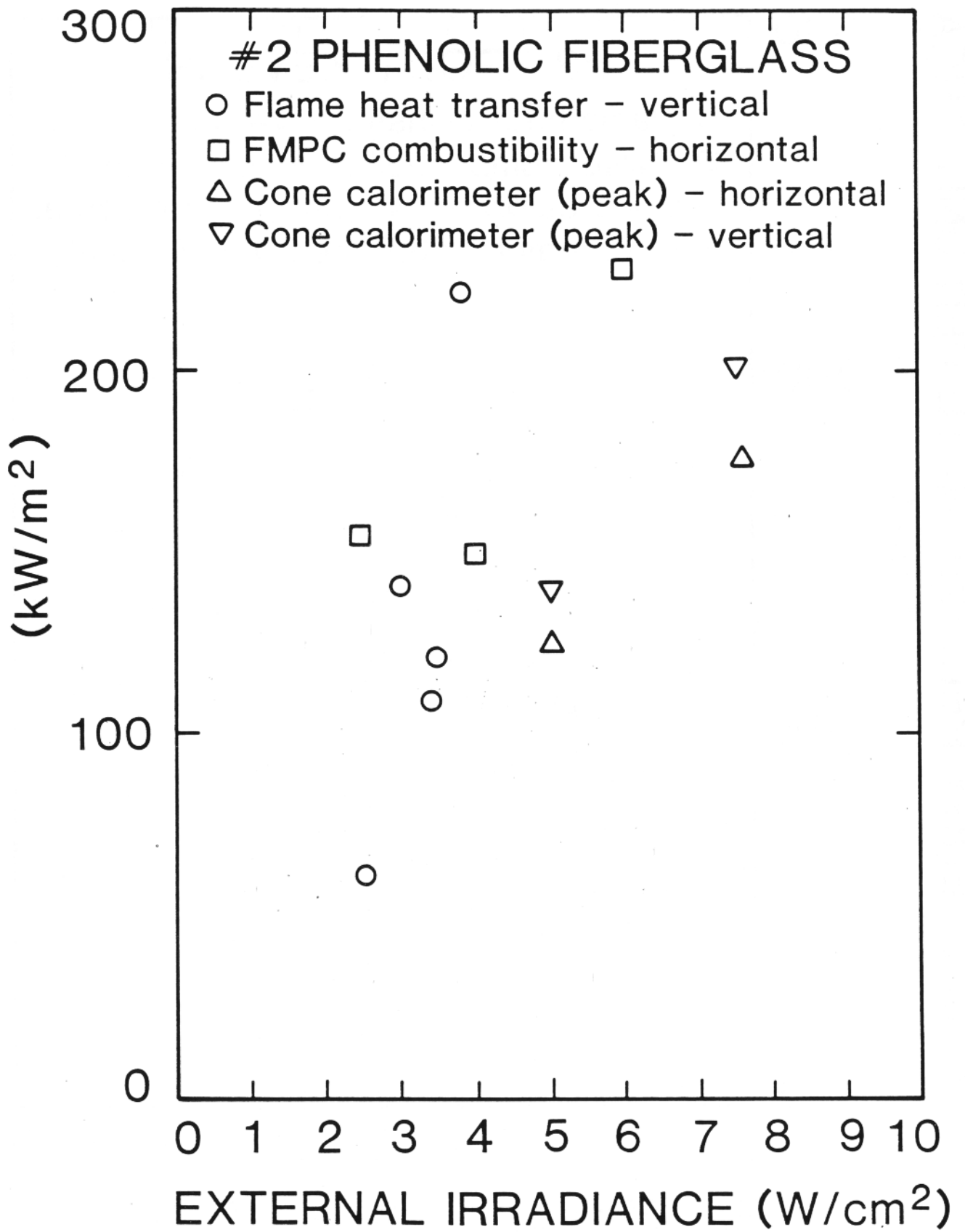


Figure 34. Peak energy release rate for phenolic/fiberglass panel.

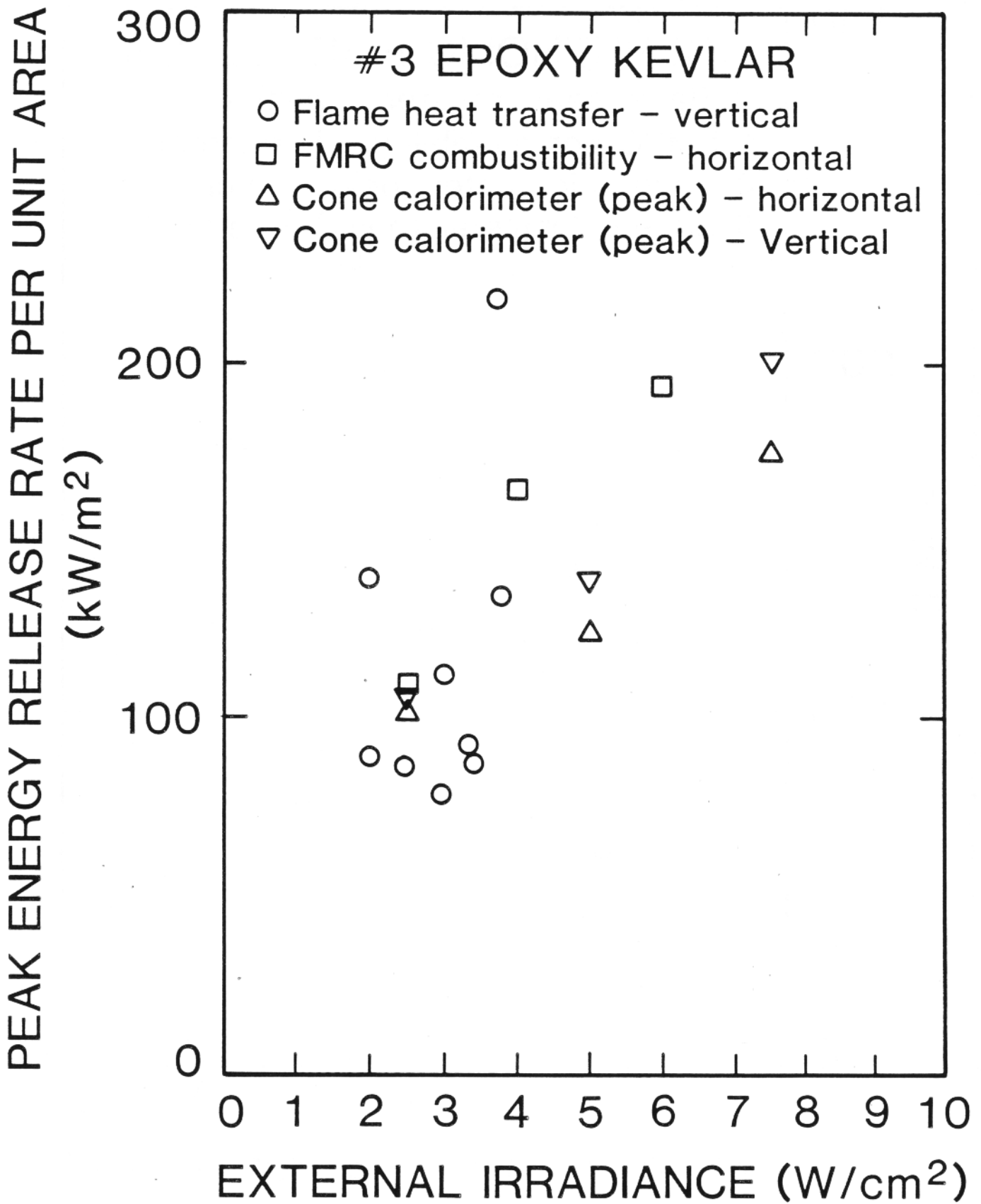


Figure 35. Peak energy release rate for epoxy/kevlar panel.

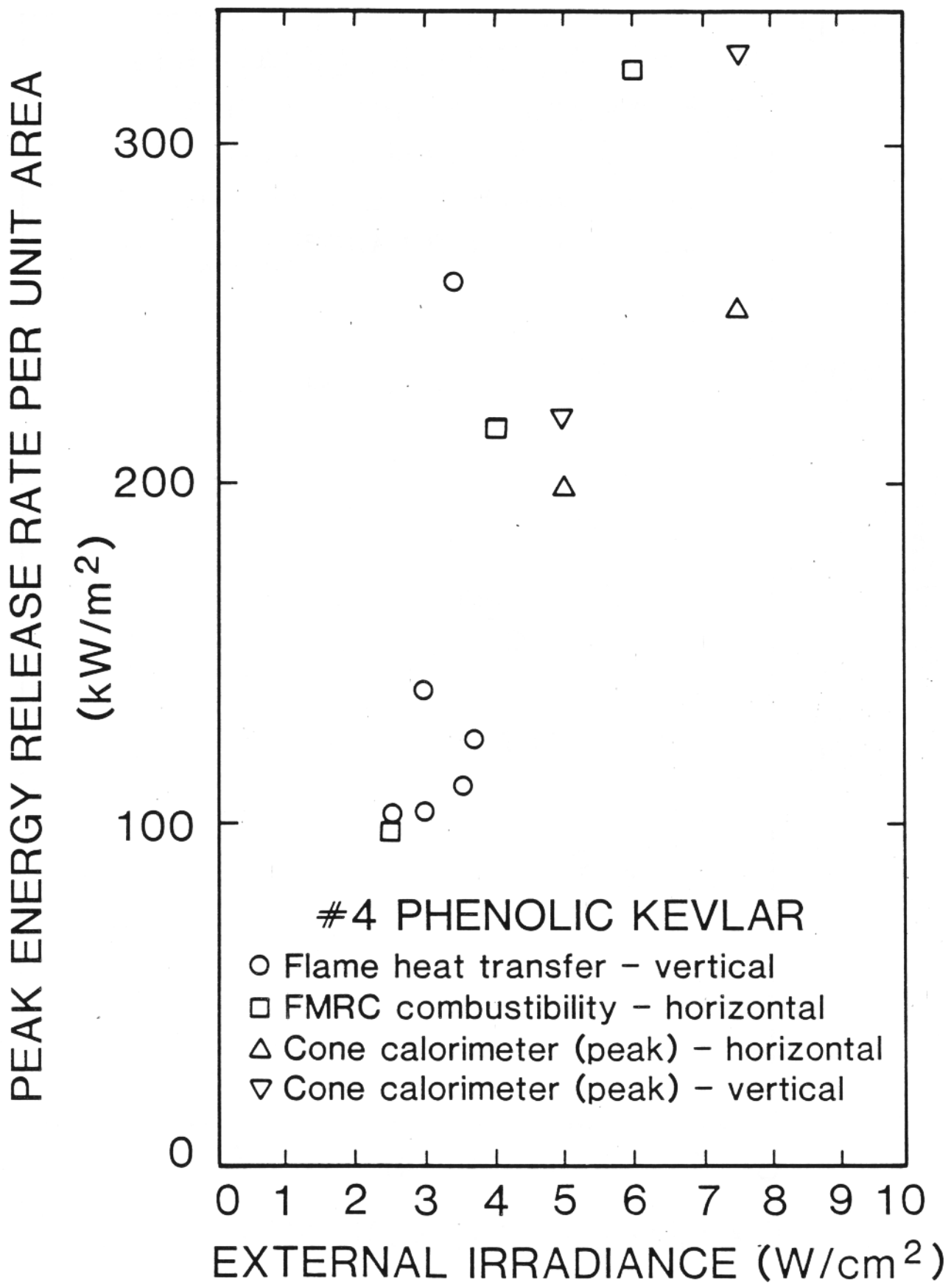


Figure 36. Peak energy release rate for phenolic/kevlar panel.

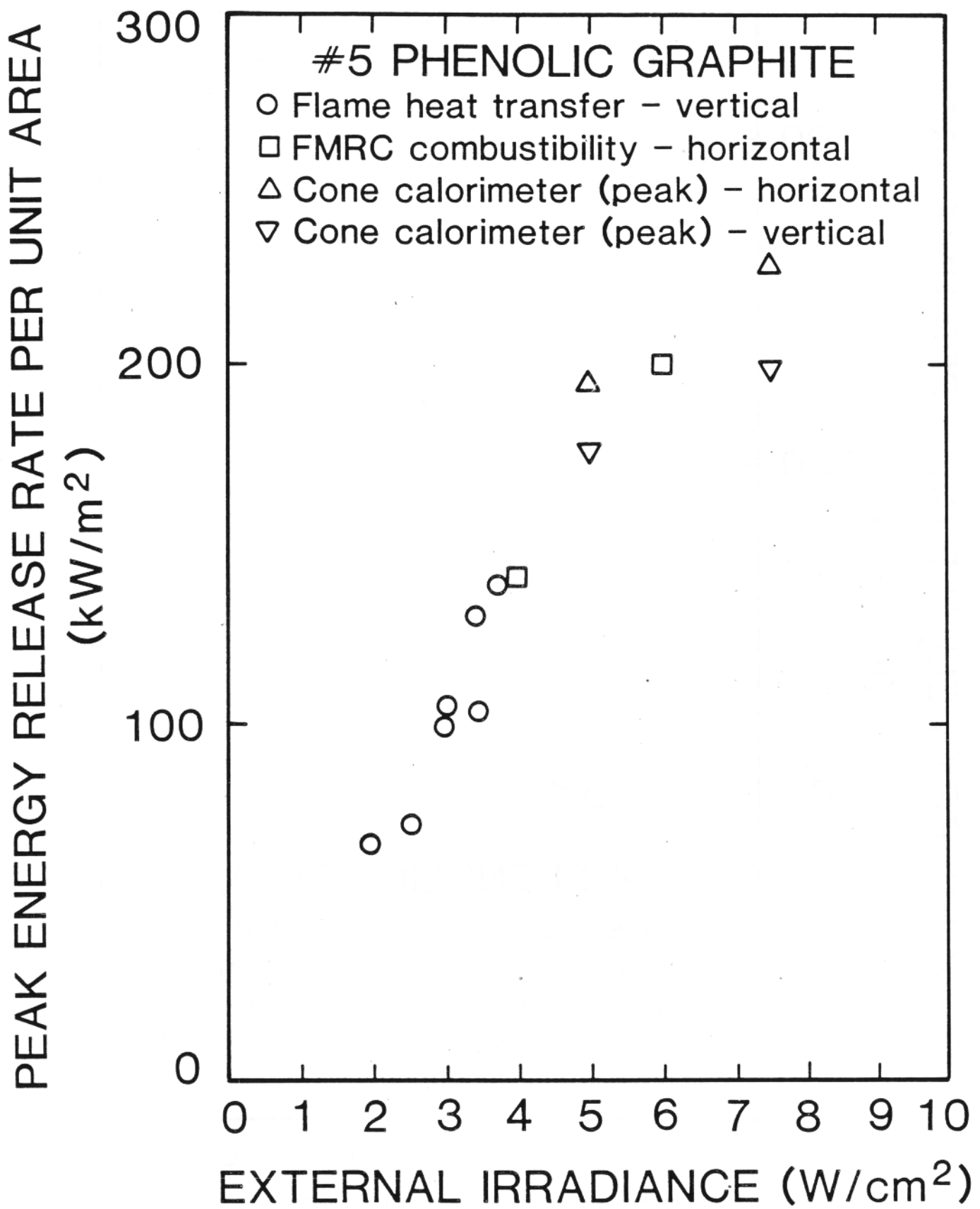


Figure 37. Peak energy release rate for phenolic/graphite panel.

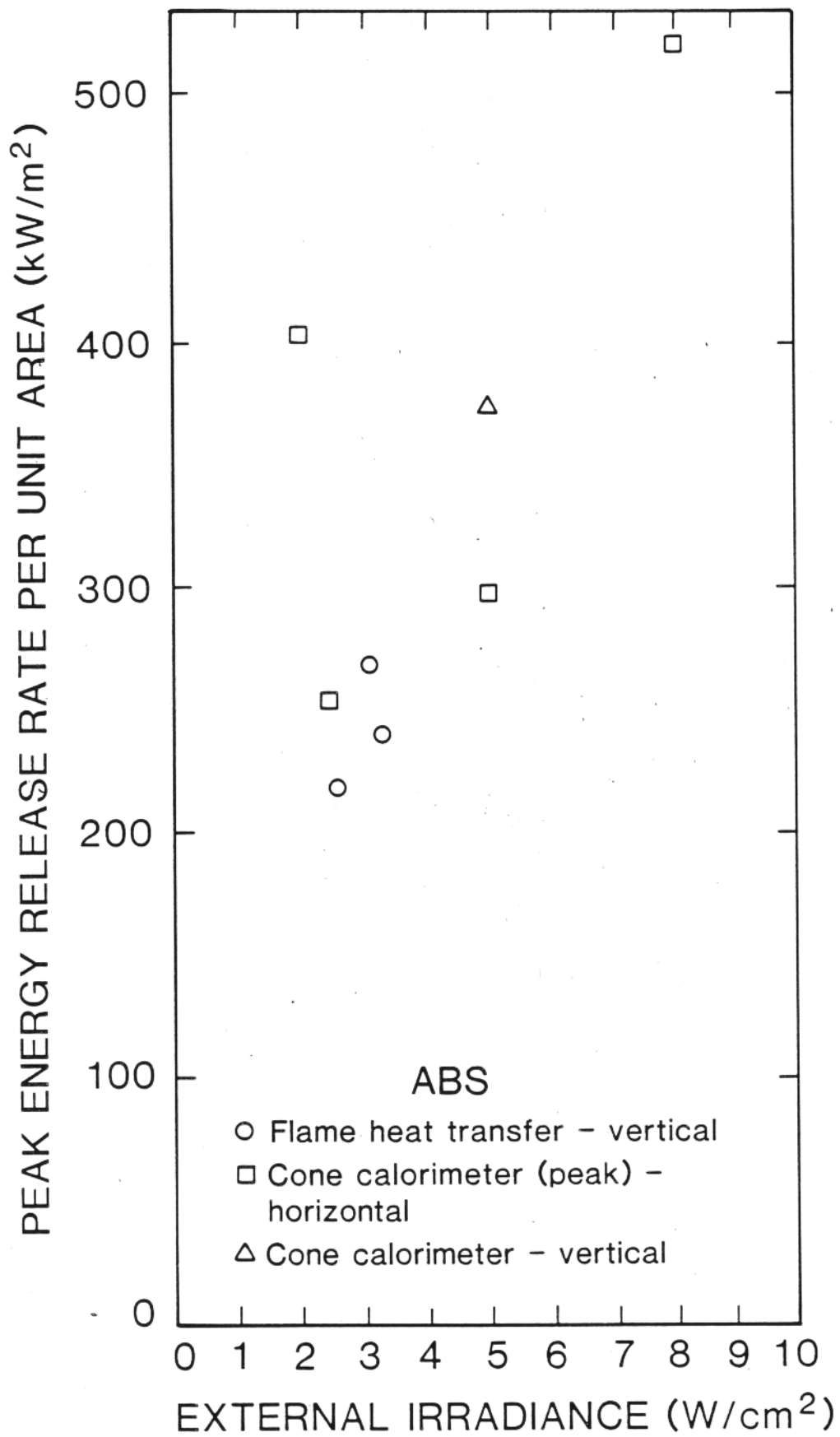


Figure 38. Peak energy release rate for ABS panel.

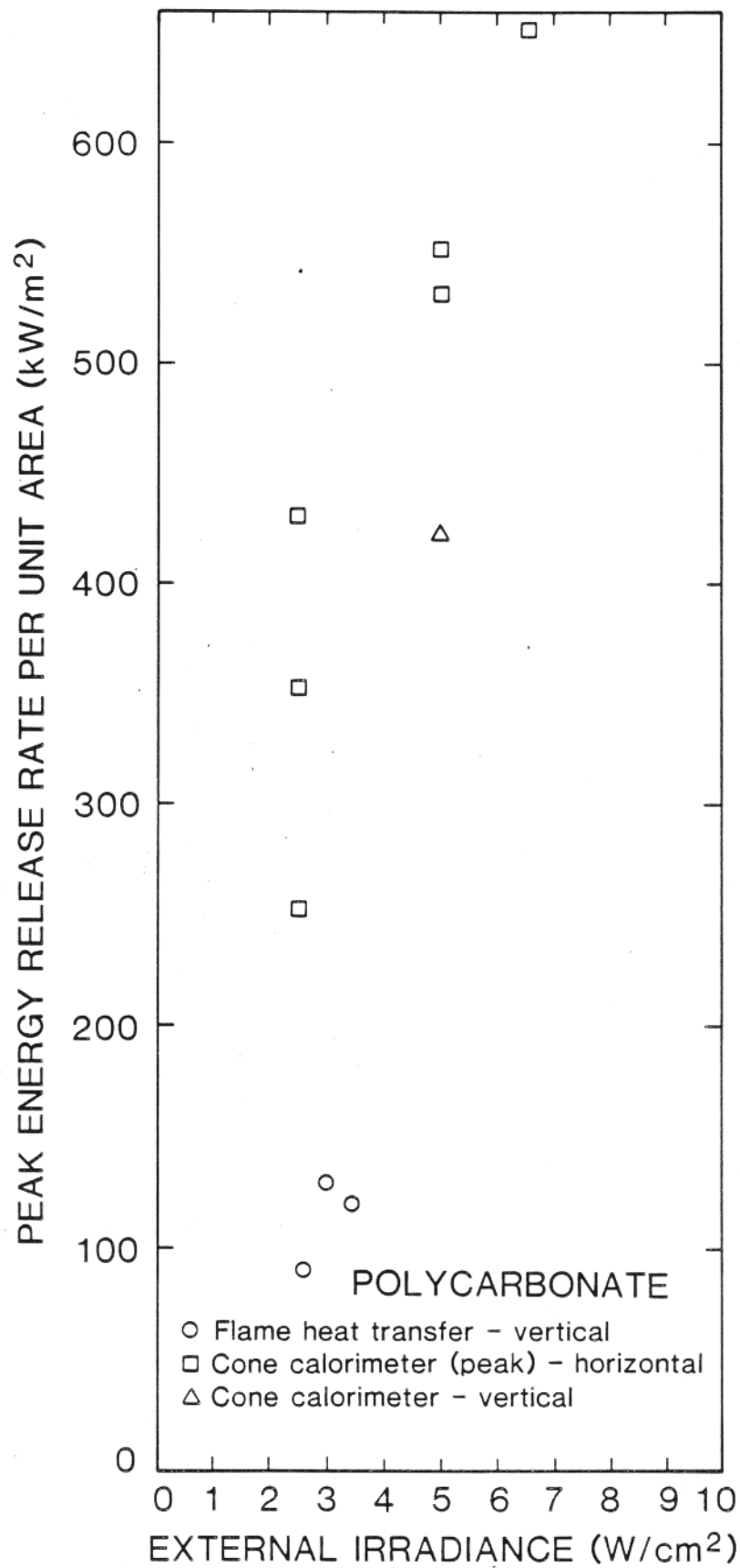


Figure 39. Peak energy release rate for polycarbonate panel.

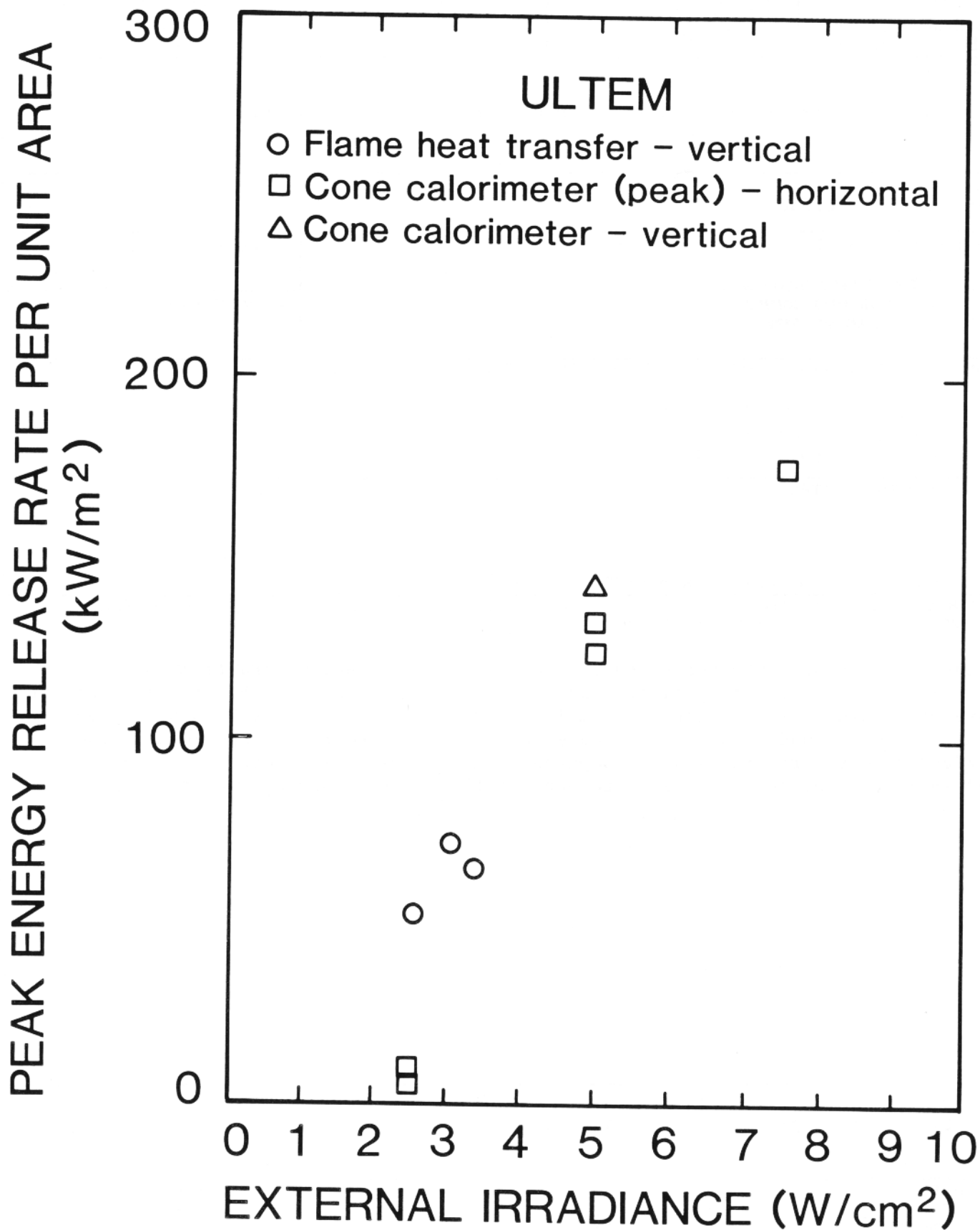


Figure 40. Peak energy release rate for ULTEM panel.

U.S. DEPT. OF COMM. BIBLIOGRAPHIC DATA SHEET <i>(See instructions)</i>	1. PUBLICATION OR REPORT NO. NBSIR 88-3773	2. Performing Organ. Report No.	3. Publication Date May 1988
4. TITLE AND SUBTITLE <p style="text-align: center;">Ignition and Flame Spread Measurements of Aircraft Lining Materials</p>			
5. AUTHOR(S) Margaret Harkleroad			
6. PERFORMING ORGANIZATION <i>(If joint or other than NBS, see instructions)</i> <p style="text-align: center;"> NATIONAL BUREAU OF STANDARDS U.S. DEPARTMENT OF COMMERCE GAITHERSBURG, MD 20899 </p>		7. Contract/Grant No.	8. Type of Report & Period Covered
9. SPONSORING ORGANIZATION NAME AND COMPLETE ADDRESS <i>(Street, City, State, ZIP)</i> <p style="text-align: center;"> Federal Aviation Administration Technical Center Atlantic City, NJ 08405 </p>			
10. SUPPLEMENTARY NOTES <p><input type="checkbox"/> Document describes a computer program; SF-185, FIPS Software Summary, is attached.</p>			
11. ABSTRACT <i>(A 200-word or less factual summary of most significant information. If document includes a significant bibliography or literature survey, mention it here)</i> <p>Experimental tests were conducted to study the lateral and upward flame spread behavior of eight aircraft lining materials. The results are tabulated in terms of parameters useful in predicting ignition and flame spread in the presence of an ignition source under exposure to an external radiant source. Experimental and derived results are graphically compared. Derived material properties related to and indicative of the propensity to support flame spread are presented.</p>			
12. KEY WORDS <i>(Six to twelve entries; alphabetical order; capitalize only proper names; and separate key words by semicolons)</i> ignition; flame spread; aircraft interiors; material properties			
13. AVAILABILITY <input checked="" type="checkbox"/> Unlimited <input type="checkbox"/> For Official Distribution. Do Not Release to NTIS <input type="checkbox"/> Order From Superintendent of Documents, U.S. Government Printing Office, Washington, DC 20402. <input checked="" type="checkbox"/> Order From National Technical Information Service (NTIS), Springfield, VA 22161		14. NO. OF PRINTED PAGES 63	15. Price \$13.95